RESEARCH ARTICLE

Influence of the industrial pollutant on water quality, radioactivity levels, and biological communities in Ismailia Canal, Nile River, Egypt

Noha Imam[1] · Amr S. El-Shamy[2] · Ghada S. Abdelaziz[2] · Dalia M. Belal[3]

Abstract

In the twenty-first century, numerous forms of pollution have adversely impacted freshwater and the entire aquatic ecosystem. The higher population density in urban areas also contributes to increased releases of substances and thermal contaminants, significantly stressing the ecosystem of industrial companies. This study aimed to assess the potential pressure of industrial and municipal activities on water quality, radioactivity levels, and biological diversity, focusing on the consequences of radionuclides on periphytic diatom communities. Furthermore, the environmental impact of pollutants will be evaluated to monitor the ecological condition of the Ismailia Canal. Chemical analyses employed various instruments and methods to identify and quantify matter, with radionuclide elements measured by gamma spectrometry and diatoms counted and identified by inverted microscopy. Our results revealed that the canal was classified as excellent for irrigation, aquatic life, and drinking water based on FAO, CCME, and EWQS water quality indices, with high nutrient levels at Abu Za'baal fertilizer company. The activity concentration of ^{226}Ra-series, ^{232}Th-series, and ^{40}K in the water and sediment samples for two seasons was within the guideline values, except for a few stations in the zone [B] (the industrial zone). Fertilizer samples (raw material) showed a high value of the ^{226}Ra-series activity. Diatom community structure significantly varied across the different canal locations regarding the presence or absence of industrial activities, with no discernible variations between the study seasons. A specific variety of algal species was found to be predominant at the highest radioactive sites. Redundancy analysis (RDA) showed a significant correlation between parameters (pH, Na, TDS, PO_4, SO_4, SiO_2, K, and CO_3), radionuclides, environmental conditions, and the composition of the diatom community, especially in the area affected by industrial discharges. Moreover, the radiological hazard index in water and sediment remained below the maximum for two seasons. This research provides valuable data and information for communities and decision-makers, suggesting the strategic use of phycoremediation as a water biotreatment process to protect the valuable economic resources of the Ismailia Canal.

Keywords Abu Za'baal industrial zone · Ecological status · Attached diatoms · Radionuclides · Environmental hazards

Introduction

The majority of industrial cities around the globe struggle with degraded water quality caused by the influx of contaminants. Industrial activities contribute substantial amounts

✉ Noha Imam
  na.imam@niof.sci.eg; nohaimam844@gmail.com

  Amr S. El-Shamy
  amrsalah1980@gmail.com

  Ghada S. Abdelaziz
  d.ghada_salah@yahoo.com

  Dalia M. Belal
  dalia_dmb@yahoo.com

[1] Physics and Geology Lab., Freshwater and Lakes Division, National Institute of Oceanography and Fisheries, 101 Kaser El Aini Street, Cairo 11516, Egypt

[2] Chemistry Lab., Freshwater and Lakes Division, National Institute of Oceanography and Fisheries, Cairo, Egypt

[3] Hydrobiology Lab., Freshwater and Lakes Division, National Institute of Oceanography and Fisheries, Cairo, Egypt

of contaminants, such as those in non-nuclear industries, including fertilizer production, coal power plants, petroleum and natural gas extraction facilities, and ceramics manufacturing (Brigden et al. 2002). The uncontrolled discharge of industrial wastewater into the aquatic system has significantly impacted the water quality and aquatic life (Begum et al. 2008). Assessing physical, biological, and chemical properties is crucial for evaluating the quality of the water class and its designated uses, including drinking, agricultural activities, and industrial purposes (Abdel-Satar et al. 2017). Industrial wastes usually comprise high amounts of dissolved and suspended substances, heavy metals, and hazardous elements (such as U, Th, and Ra) that may influence the ecology of aquatic organisms, interrupting the entire system and posing direct or indirect threats to human health (Pappa et al. 2016). Additionally, they affect the biodiversity of aquatic biological communities, such as the richness and evenness of species (Li et al. 2022). Environmental stresses may result in declines in diversity or changes in the abundance of aquatic biological communities, while biodiversity metrics assist in describing the numbers and distributions of species (Li et al. 2022).

Environmental pollution is undoubtedly one of the main problems that society faces today. Periodic water quality surveillance in the aquatic ecosystem is essential to assess ecological health and suitability for various purposes, such as agriculture, industry, and domestic (Poonam et al. 2013). For instance, raw materials for producing fertilizers include considerable amounts of natural radionuclides. The manufacturing process of these materials may expose staff members and nearby residents to radiation levels significantly higher than background radiation (Righi et al. 2000). Earlier studies have reported significant activity concentrations of radionuclides such as ^{238}U, ^{232}Th, and ^{226}Ra in fertilizers and the area around fertilizer plants (Bolivar et al. 2000). Natural radionuclides are present in various geological formations, such as soil, water, sediments, and building materials widely distributed in the environment. When rocks undergo natural processes, radionuclides are transported to the soil by rainfall and run-off (Taskin et al. 2009). However, some rocks are found at higher concentrations than others; for example, felsic igneous rocks are found at higher concentrations than sedimentary rocks (Bastos and Appoloni 2009).

Radioactive contamination, occurring when radionuclides are discharged into an aquatic system and eventually settle to the bottom by sorption on suspended solids, stands out as one of the most hazardous forms of pollution (Eisenbud and Gesell 1997). However, it is necessary to understand the water body's morphology, the ecological significance of aquatic systems concerning environmental variables, particularly the distribution of species and variety and the influential relationship between the various parts of the food chain. Diatoms, an important category of primary producers

in aquatic ecosystems and an essential component of the phytobenthos, are excellent indicators of eutrophication. They are also radionuclide indicators in aquatic ecosystems (Pradhan and Sukla 2019; Banerjee et al. 2022).

The Ismailia Canal, which crosses between residential areas and some factories, is considered one of the crucial branches of the Nile in Egypt. However, several sources of pollution influence the Ismailia Canal's water quality (Geriesh et al. 2008), owing to several effluents that can significantly alter the chemical and physical characteristics of the River Nile and its canals. This, in turn, affects the ecological status of river breaches (El-Sayed 2011) and may change the radionuclides concentration in this area (Abdel Malik et al. 2010). Due to these circumstances, continuous monitoring of the ecological characteristics and radioactivity levels of the water in the Ismailia Canal is essential to ensure its safety. Therefore, the current study aimed to assess the water quality, the radioactive contamination in water and sediments, and the biodiversity of primary producers presented by the attached diatoms. This evaluation seeks to evaluate the potential of diatoms for bio-indication in the Ismailia Canal. Furthermore, the study aims to calculate the environmental impact and hazard indices of industrial pollutants in the water body of the canal. This monitoring is crucial to determining the variation of environmental characteristics and radioactivity levels resulting from the industrial effluents in the Ismailia Canal.

Materials and methods

Study area

The Ismailia Canal is one of Egypt's crucial irrigation and water resources. It was built in 1862 to supply drinking water to the cities in the Suez Canal area. Stretching approximately 125 km, it is located east of the Nile at Shupra, north of Cairo. Characterized by a depth ranging from 1 to 3 m and a width ranging from almost 30 to 70 m, with a mean water flow of 0.28 m/s (Geriesh et al. 2008) (Fig. 1). The canal passes through different geologic formations, including silt and mud on its upstream west bank and sand and marl on its downstream east bank (El-Mathana et al. 2021). Around 12 million Egyptians rely on it as their primary source of drinking water and irrigation (Geriesh et al. 2008). The outflow of the canal is about 5,000,000 m^3 of water daily for drinking, irrigation, and industrial purposes (El-Haddad 2005). Major industrial zones line the upstream section from Cairo to Abu Za'baal (Shupra El Kheima, Musurod, and Abu Za'baal industrial zones). Notably, at the field scale, Al Delta Company for Iron, the Electro Cable Egypt Company (ECE), the Petroleum Company and the Aluminium Sulfate Company serve as point sources of pollution. The Abu Za'baal
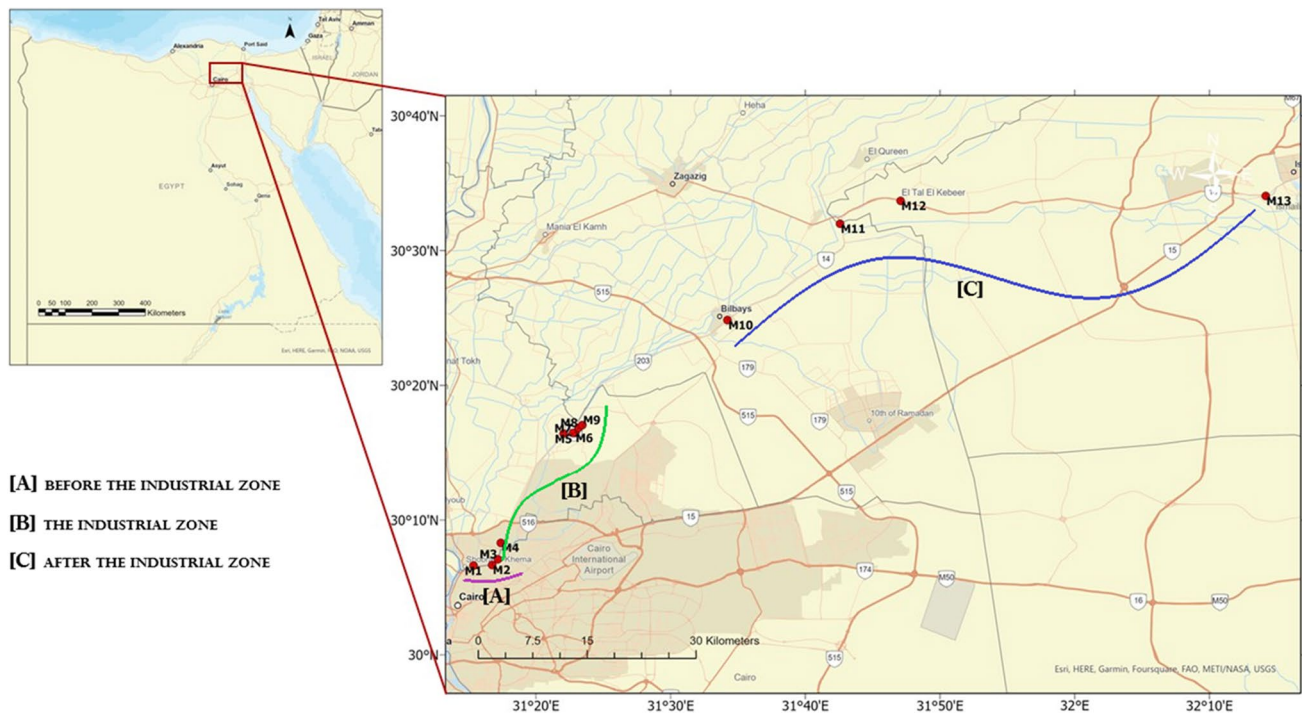
Fig. 1 Location map of the sample sites at Ismailia Canal

Fertilizers Company acts as a point and non-point source of pollution. In the area from Abu Za'baal to El-Ismailia along the canal's banks, many agricultural run-offs are classified as non-point sources of contamination. Toxic metals and wastes from factories and residential areas enter the canal. Farmers employing many fertilizers also risk leakage into the River Nile, its canal, and its branches (Manigandan and Chandar Shekar 2014). Superphosphate and rock phosphate stand as the primary sources of phosphate fertilizers used in agricultural production in Egypt, with the recent adoption of alternatives like phosphoric acid for production (Mohamed 2021). According to Atlas, the average annual rate of fertilizer use in Egypt has increased by 3% per hectare from the 1970s to the 2020s. An elevated level of some toxic metals, such as cadmium and lead, surpassing permissible limits in the surface water of the Ismailia Canal, may be attributed to the waste of electric batteries, electronic components, and industrial wastes (Ibrahim et al. 2014). Indeed, the industrial discharge pipes of the Abou-Zabal (AZ) Company, sulfate of aluminium and potassium (alum, p), iron and steel companies, and ceramic factories constitute point sources of contamination.

Sampling collection and preparation

The sediment and water sampling strategy involves selecting points at the pollution discharge site, downstream and upstream of the discharge. The sediment and water samples were collected from 13 locations, as described in Table 1, along the length of the Ismailia Canal. Three samples from each of these sites were carefully selected and intended to be representative of each site. Environmental parameters, including pH value, electrical conductivity, and water temperature, were measured in situ using the Hydrolab model (Multi Set 430i WTW). A Secchi disk (30 cm in diameter) was used to measure transparency.

Regarding the radioactivity measurements, bottles were washed with diluted HCl acid to prevent radioactive materials from precipitating on the surface. The samples were collected using a water sampler in a 5-l polyvinyl chloride plastic container without filtration and stored in an icebox until we returned to the lab. Surface sediment is sampled using an Ekman grab sampler (15 cm × 15 cm, 225 cm^2), quickly packed in airtight polythene bags, and stored in an ice box at the site. The sediment samples would be crushed, dried at 70 °C, and sieved to a mesh size of 63 mesh. Commercial fertilizer samples were collected from the local market, and raw materials were obtained from the Abou-Zabal (AZ) Company. Sampling occurred during the winter and summer of 2022 (M1-M13) (Fig. 1, Table 1). For diatom examination, epipelic samples were taken from the sediment's surface layer (nearly 1 cm or within the first millimetres), where most benthic diatoms are present. This community was quantitatively collected by inserting a spatula into glass vials under a defined sediment surface area to a depth of 2 cm.

Table 1 Details, latitude, and longitude of sampling locations

Sample code		Site location	Site descriptions	Latitude	Longitude
Before the industrial zone [A]	M1	El Mazalate (Mouth of Ismailia Canal)	Around the civilization area in the vicinity of Cairo	30° 06′ 628″	31° 15′ 365″
	M2	Close to Al-Amiria Water Treatment Plant	Received the discharge of waste water from the water treatment plants	30° 06′ 672″	31° 16′ 744″
The industrial zone [B]	M3	Mostourd (Izbat El Rayse) (in front of Al Delta company for Iron, Electro Cable Egypt Company (ECE))	Received the industrial waste from the company of the power cables and telecommunication cables as well as metal wires	30° 07′ 097″	31° 17′ 165″
	M4	Downstream of Petroleum Company (Drain)	Received the industrial waste from direct discharge of petroleum and natural gas activities	30° 08′ 315″	31° 17′ 398″
	M5	Upstream of Abu Za'baal fertilizer Company	Received atmospheric deposition from dust from the Abu Za'baal Fertiliser Company, industrial waste of the company and agricultural run-off	30° 16′ 094″	31° 22′ 043″
	M6	In front of Abu Za'baal fertilizer Company	Received atmospheric deposition from dust from the Abu Za'baal Fertiliser Company, industrial waste of the company and agricultural run-off	30° 16′ 466″	31° 22′ 887″
	M7	Downstream of Za'baal fertilizer Company (Drain)	Received atmospheric deposition from dust from the Abu Za'baal fertilizer company, industrial waste of the company and agricultural run-off	30° 16′ 471″	31° 22 741″
	M8	Close to Aluminum Sulfate Company (Drain)	Received the chemical waste from the Aluminum Sulfate Company and agricultural run-off	30° 16′ 843″	31° 23′ 165″
	M9	Downstream of Aluminum Sulfate Company	Received the chemical waste from the Aluminum Sulfate Company and agricultural run-off	30° 17′ 050″	31° 23 443″
After the industrial zone [C]	M10	Bilbeis	Agricultural run-off	30° 24′ 840″	31° 34′ 225″
	M11	Al Abbas	Agricultural run-off	30° 31′ 984″	31° 42′ 576″
	M12	El-Tal El-Kabee	Agricultural run-off	30° 33′ 690″	31° 47′ 068″
	M13	El-Ismailia (before bifurcation)	Agricultural run-off	30° 34′ 057″	32° 14′ 178″

Chemical analysis

Water samples were stored in 26 polyethylene bottles in an ice box for laboratory analysis. The American Public Health Association (APHA, American Public Health Association 1995) explained how to determine most physicochemical parameters. The total dissolved solids (TDS) were determined by filtrating a sample volume with a glass microfiber filter (GF/C), and a known filtrate volume was evaporated at 105 °C. The total suspended solids (TSS) were measured by the filtration of a specific sample volume and subtraction of the TS-TDS. Total solids (TS) were determined by the evaporation of a certain amount of sample that had been well mixed. The modified Winkler method measured dissolved oxygen (DO), while chemical oxygen demand (COD) was estimated according to the potassium permanganate method.

A 5-day method was used to determine biochemical oxygen demand (BOD). Transparency was measured using a white/black Secchi disk (25 cm in diameter) and expressed as the Secchi disk depth (SDD). Various parameters, including pH, temperature (°C) of water, and conductivity (EC, µS/cm), were in situ measured using a hydrolab model (Multi Set 430i WTW, Weilheim, Germany) after previous calibration. The chloride content was determined using the Mohr method, and the sulfate content was determined by the turbidimetric method. Indicators such as methyl orange and phenolphthalein were used to measure water alkalinity immediately after sampling. Magnesium and calcium were measured by direct titration in an EDTA solution, and K^+ and Na^+ were measured using a 'Jenway PFP7 UK flame photometer. A blank and calibration standard curve was prepared in a stepped amount in the following applicable

ranges: 1, 2, 5, 100, and 200 mg/l, with concentrations deduced from the calibration curve from a series of standard solutions. A Jenway 6800 double-beam spectrophotometer, UK (scan in the range 190 to 1100 nm with resolutions up to 0.1 nm and scan speeds up to 3600 nm/s) and colorimetric methods were used to measure NO_2-N, NO_3-N, NH_4-N, PO_4-P, and SiO_4 concentrations. Total phosphorus (TP) was determined as reactive phosphate after persulfate digestion. All solutions and chemicals used in this study were of the highest purity (Sigma-Aldrich Analytical Grade).

Radioactivity measurements

Non-destructive sodium iodide gamma spectrometry using a 2×2 NaI(Tl) setup and a multichannel analyser (MCA) was used to measure radioactivity in the samples (water and sediment): The resolution (FWHM) is 24.22 keV at 1.33 MeV ^{60}Co, and the relative efficiency is 7% with a lead shield to reduce the background. The sample was on the detector for at least 72 h, and the spectra were analysed manually with a spreadsheet (Microsoft Excel) for radionuclide determination and automatically with the Maestro computer program (EC&G ORTEC). The daughters (^{214}Pb and ^{214}Bi) were used to determine the activity concentration of the ^{238}U(^{226}Ra) series over 295.1 keV and 352.0 keV for ^{214}Pb and 609.3 keV, 1120.3 keV, and 1764.5 keV for ^{214}Bi. The activity concentration of the ^{232}Th series was calculated using the gamma energy lines 911.2 keV and 969.11 keV for the ^{228}Ac and 2614.4 keV for the ^{208}Tl and 239 keV for the ^{212}Pb and using the direct gamma energy line 1460.8 keV for the measured ^{40}K (Chieco et al. 1990). The calibration of the detector efficiency was performed via the IAEA standard sources RGU-1, RGTh-1, and RGK-1 (IAEA 1987). The IAEA-certified reference materials (IAEA-443, IAEA-446, IAEA-410, and IAEA-312) are used to perform quality control (QC) procedures to verify the reliability and precision of the experimental results reported in this study (Appendix Table 10). After that, the samples were stored for at least 4 weeks in sealed beakers. This ensured that there was no radon loss and that radium isotopes and their daughters had reached a secular equilibrium. The activity concentrations of the radionuclides, expressed as becquerels per kilogram for sediment and becquerels per litre for water samples, were determined using the formula developed by El Afifi et al. (2006). The precision of the gamma spectrometer is determined by the lowest detection limits (LLDs) of the measuring system (USDOE 1992). The LLD values obtained for ^{40}K, ^{226}Ra, and ^{232}Th were 8, 1, and 1 Bq/kg, respectively, for the sediment samples and 0.5, 0.04, and 0.05 Bq/l, respectively, for the water samples. The uncertainty of activity, U_{AC}, is calculated from uncertainty of components C, P, and W as follows (Asaduzzaman et al. 2016):

$$U_{AC} = \sqrt{\lceil \frac{U_C}{N_C} \rceil^2 + \lceil \frac{U_\varepsilon}{\varepsilon} \rceil^2 + \lceil \frac{U_p}{P} \rceil^2 + \lceil \frac{U_w}{W} \rceil^2} \quad (1)$$

where U_C, U_ε, U_P, and U_W are respective uncertainties for the net count per second, the detector efficiency, the gamma decay transition probability, and the sample mass.

Diatom sample preparation and laboratory analysis

After adding tap water, the preserved samples were placed in a 500-ml beaker and vigorously stirred for a few minutes. Heavy clay and sand particles were allowed to settle in the samples briefly following stirring. At the same time, the supernatant fluid containing microalgae was put into a cylinder with a capacity of 1 l. This process was repeated at least six to eight times. A few drops of an acidic solution of iodine were also added. The samples were concentrated to make 100 ml of samples in plastic bottles. Homogenized samples, consisting of 0.5 g of clay sediment and approximately 2 g of sandy sediment, were subjected to concentrated nitric and sulfuric acid treatments. The samples were heated until all organic matter was oxidized, according to ANS (2002), for further identification confirmation. Samples were neutralized by repeated washing and concentration (Belal 2012). Utermohl (1958) approach was employed for diatom counting and identification using an inverted microscope (Zeiss, Model Axiovert 25C). Primary sources for identifying epiphytic diatoms included Cleve-Euler (1953), Patrick and Reimer (1975), and Krammer and Lange-Bertalot (1986, 1988, and 1991).

Environmental impact and hazard indices

Water quality index (WQI)

The water quality of the Ismailia Canal was assessed using the CCME-WQI module and calculated using the following equation (CCME 2001):

$$CWQI = 100 - \frac{\sqrt{F_1^2 + F_2^2 + F_3^2}}{1.732} \quad (2)$$

F_1 (scope) is the percentage of variables that do not meet their objectives at least once during the considered period (failed variables). F_2 (frequency) is the percentage of individual tests that do not satisfy their objectives. F_3 (amplitude) represents the amount of failed test values that do not meet their targets. Water quality is classified according to one of the categories outlined in Appendix Table 11. The guidelines from the Egyptian Drinking Water Quality Standards (2007) were used to calculate the WQI for drinking water. The WQI for irrigation water was calculated

following the FAO (1994) guidelines. Additionally, the guidelines of CCME 2007 were used to calculate the protection of aquatic life. Detailed water quality guidelines are illustrated in Table 2.

Radiation hazard indices

Safely assessing the health risks of exposure to humans or the environment requires using many standard radiation hazard indices. The estimated indices include the absorbed dose rate in the air (D) (UNSCEAR 2000), annual effective dose rate (AED) (UNSCEAR 2000), radium equivalent activity (Ra_{eq}) (Kurnaz et al. 2007), the external hazard index (H_{ex}) (UNSCEAR 2000), and the representative level index ($I\gamma$) (Chad-Umoren and Umoh 2017). The calculations for these indices are detailed in Appendix Table 12. To estimate the total risk assessment of consumed water, it is crucial to consider the health impacts of the hazards connected to all radium isotopes, such as the cancer risk (EPA 1999; Abdellah and Diab

2012) and the effective radiation (DRW) (USEPA 1999), using the equations provided in Appendix Table 12. These assessments are essential for determining any potential health risks.

Statistical and data analysis

The correlation between diatom diversity, richness, evenness, and physicochemical and radionuclide properties was assessed by calculating the Pearson correlation coefficient using Primer software version 5 (Clarke and Gorley 2001). The Pearson correlation coefficient (r) quantifies the strength of a linear association between diatoms (richness, evenness, and diversity) and the physicochemical and radioactive elements. This analysis aimed to determine whether these measured variables influenced the components of the diatom communities in the Ismailia Canal. A redundancy analysis (RDA) was also performed as a constrained ordination to ascertain how variance in the diatom community composition could be explained

Table 2 Mean, standard deviation and range of water parameters compared to guidelines used in WQI

Parameters	Range	Mean ± SD	CV %	Drinking water		Irrigation[3]	Aquatic life[4]
				Egypt[1]	WHO[2]		
Temp, °C	15.30–37.22	24.41 ± 7.19	29.48			< 35	8.0–28.0
Trans, cm	40–140	86.67 ± 31.44	36.27				
EC, mS/cm	293–530	373.08 ± 74.50	19.97	2000		3000	
pH	7.31–8.2	7.83 ± 0.22	2.85	6.5–8.5	8.5	8.5	6.5–9
TDS, mg/l	175–317.8	225.79 ± 43.15	19.11	1000	500	2000	< 500
TSS, mg/l	9.22–69	33.12 ± 14.17	42.79				25
TS, mg/l	307.30–534	391.38 ± 56.40	14.41				
DO, mg/l	2.8–7.10	5.38 ± 1.03	19.13	6		> 4	> 5.5
BOD, mg/l	0.40–5.80	2.62 ± 1.69	63.33	3			< 6
COD, mg/l	2.00–12.40	5.15 ± 2.89	55.98	10	10		7
NH$_4$, µg/l	107.64–157.68	134.98 ± 14.10	10.45	450	200	5000	1370
NO$_2$, µg/l	0.012–9.91	3.01 ± 2.29	76.02	5	900		60
NO$_3$, µg/l	81.37–198.36	142.01 ± 31.56	22.23	10,000	11,000	10,000	2930
PO$_4$, µg/l	24.23–407.85	77.41 ± 100.10	129.32			2000	
TP, µg/l	137.22–524.25	237.01 ± 96.61	40.76	1000			
SiO$_4$, mg/l	0.58–5.43	2.34 ± 1.47	60.65				
CO$_3$, mg/l	0.00–10.47	7.20 ± 3.38	47.00			3	
HCO$_3$, mg/l	143–185.11	159.49 ± 10.86	6.81			610	
Cl, mg/l	26.99–31.99	28.15 ± 3.44	12.21	250	200	1063	120
SO$_4$, mg/l	26.55–79.19	36.71 ± 13.16	35.83	250	250	960	
Ca, mg/l	16.03–21.64	18.62 ± 1.31	7.03	75	75	400	
Mg, mg/l	4.86–9.73	7.24 ± 1.38	19.03	50	50	60	
Na, µg/l	22.45–34.66	27.81 ± 3.44	12.35	200		919	
K, µg/l	6.5–9.36	7.92 ± 0.85	10.72			2	

[1]Egypt (2007)
[2]WHO (2011)
[3]FAO (1994)
[4]CCME (2007)

by the variation in the measured chemical, physical, and radioactive elements. Using Canoco Windows version 4.1 (Ter Braak 1987), the relative abundance of frequently recorded diatom taxa ($\geq 30\%$) was incorporated alongside environmental variables. The Canoco 4.5 software (Ter Braak and Smilauer 2002) was used to perform the discriminant analysis (DA) and the redundancy analysis (RDA) of the physicochemical variables, nutrient salts, and significant elements for the different locations, including the radioactive elements in the Ismailia Canal. A Monte Carlo permutation test with 499 permutations was set to identify the significant environmental variables, major elements, and nutrient salts influencing the distribution of radioactive elements ($P < 0.05$).

Results and discussion

Chemical analysis

Table 2 illustrates water quality parameters. The data shows low regional variations in water temperature, except in thermally polluted regions such as station (3), which recorded the highest summer temperature of 37.22 °C. Transparency was affected by the industrial effluent discharge, particularly at stations 2, 4, 6, and 8 varying between 40 and 140 cm, with a highly significant geographical and temporal variations ($P < 0.01$). In the present study, transparency exhibited a negative correlation with TSS and TDS, which agrees with those reported by Goher et al. (2014), who reported similar negative associations between cations and anions, TSS and TDS, and transparency in Ismailia Canal water. It was noticed that an increase in the canal's flow rate led to an increase in the water level, causing sediment agitation, an elevation in the concentration of TSS, and, consequently, a decrease in the water's transparency. A high temporal difference ($P < 0.01$) was noted for TSS and TDS.

The pH ranged from 7.31 to 8.2, remaining within the limits for drinking water and aquatic life guidelines in two seasons (Abdel-Aal et al. 2023). Elevated electrical conductivity (EC) values were observed at the stations (2, 4, 6, and 8) nearest the industrial discharges, while lower values were observed at the stations upstream and downstream of the pollution sources. In the winter, the lower water level of the Ismailia Canal led to increased ions concentration, raising the EC level, which agrees with the results obtained by Hussein et al. (2023), Talab et al. (2016), and Goher et al. (2015) in the Nile River, the El-Rayah of Nile, and El-Bahr El-Pharaony, respectively. TDS levels are negatively correlated with water flows, with winter recording the highest levels and

summer recording the lowest levels (high dilution). El Sayed et al. (2023) and Goher et al. (2014) reported that bicarbonate is the leading cause of the Ismailia Canal's total alkalinity. Highly significant variations ($P < 0.01$) in bicarbonate alkalinity were observed between the sampling seasons. At the same time, spatial variation ($P < 0.05$) was recorded along the sampling sites of the canal, except for the polluting point sources (2, 4, 6, and 8). A negative significant correlation ($r = -0.66$, $n = 26$) ($P < 0.05$) was observed between HCO_3^- and silicate concentrations, potentially attributed to algal uptake of CO_2, with silicate and CO_2 being absorbed by diatoms (Wang et al. 2013). Dissolved oxygen (DO) is critical for assessing the water conditions for aquatic life and drinking water (El Sayed et al. 2020). Mean DO values remained within the limits recommended by CCME (2007) for aquatic life at all sites except station (10) (in front of the source of domestic waste). The BOD and COD values showed significant spatial variations ($P < 0.01$), ranging from 0.40 to 5.80 mg/l and 2.00 to 12.40 mg/l, respectively. BOD and COD are generally indicators of organic pollution (Elsayed et al. 2019; Goher et al. 2021). The discharge of industrial effluents was responsible for the maximum COD value measured at the station (8) during two seasons, consistent with the results obtained by Hussien et al. (2023) in the Nile River, El Sayed et al. (2023) in the Ismailia Canal, and Talab et al. (2016) in the Nile Rayahs.

The distribution of chloride and sulfate exhibited significant temporal differences ($P < 0.01$), with significant increases at the site (6), consistent with the findings of Abdo and El-Nasharty (2010). Sulfate and chloride have a positive correlation with Ca^{+2} and Mg^{+2}. Calcium and magnesium values varied from 16.3 to 21.64 and 4.86 to 9.73 mg/l, respectively, with a substantial seasonal variation ($P < 0.01$).

Calcium and magnesium concentrations were at their lowest during the summer season. This could be attributed to the adsorption of clay minerals and deposition on the bottom due to temperature increases, as El Bouraie et al. (2010) suggested, and the consequences of the flood period. Sodium and potassium levels were recorded at 22.45–34.66 and 6.5–9.36 mg/l, respectively, with significant variations between sites and seasons ($P < 0.01$). Nutrient salts were within the ranges of 0.012–9.91, 81.37–198.36, 107.64–157.68, 24.23–407.85, 137.22–524.25 µg/l, and 0.58–5.43 mg/l for nitrite, nitrate, ammonia, orthophosphate, total phosphorus, and silicate, respectively. The highest concentrations of nutrient salts were found at the site (6), likely attributed to the industrial effluents discharged.

[A] Before the industrial zone

[B] The industrial zone

[C] After the industrial zone
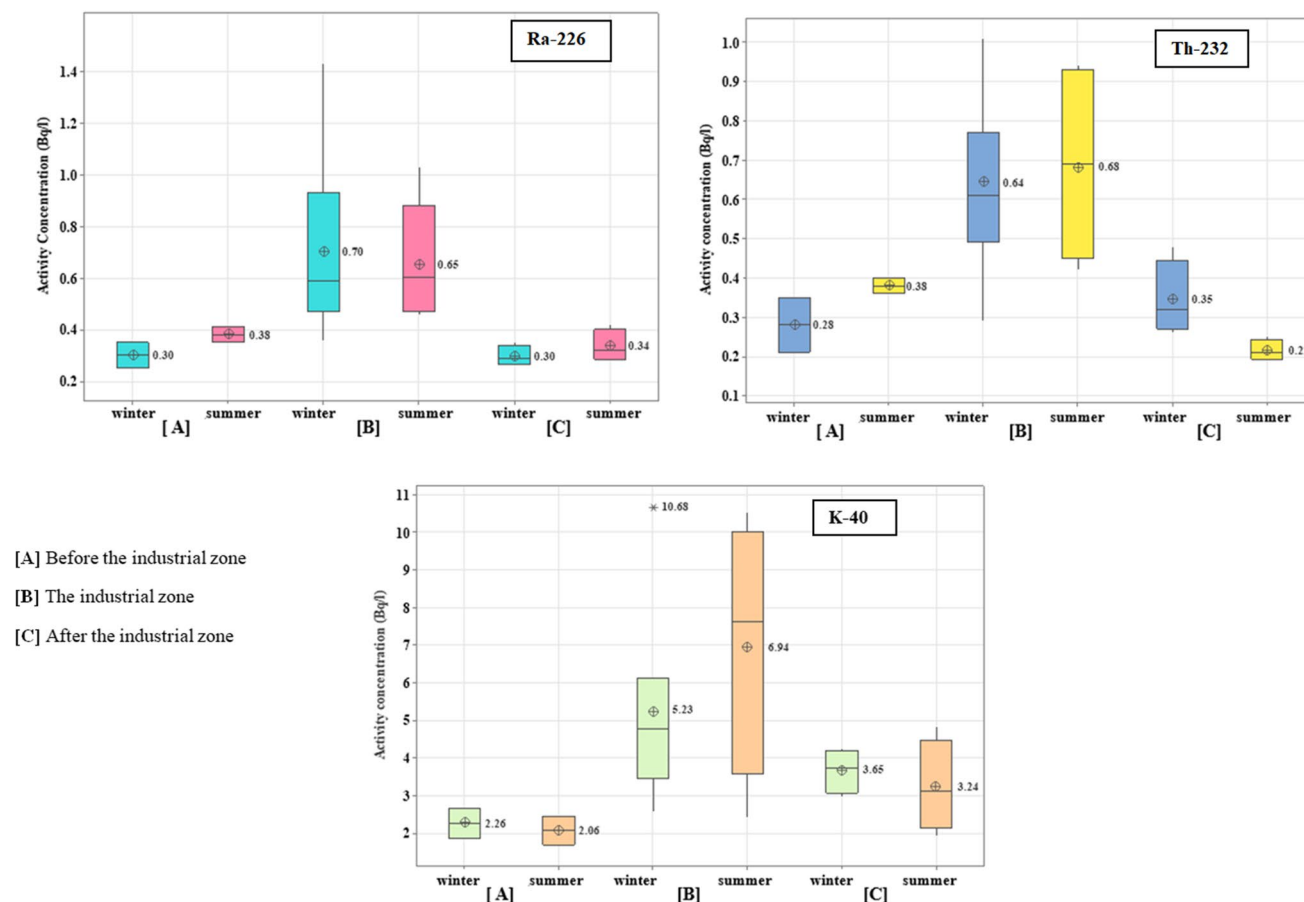
Fig. 2 The distribution of ^{226}Ra-series, ^{32}Th-series, and ^{40}K in water samples of Ismailia Canal

Radioactivity measurement

Water

The activity concentration of Ra-226 series, Th-232 series, and K-40 in water samples during the winter and summer seasons is presented in Fig. 2 and Table 3. In winter, the specific activity of ^{226}Ra, ^{232}Th, and ^{40}K varied from 0.25 ± 0.05 to 1.43 ± 0.22 Bq/l, 0.21 ± 0.09 to 1.01 ± 0.16 Bq/l, and 1.85 ± 0.25 to 10.68 ± 1.39 Bq/l, respectively. In summer, the range was 0.28 ± 0.04 to 1.03 ± 0.14 Bq/l, 0.19 ± 0.02 to 0.94 ± 0.05 Bq/l, and 1.67 ± 0.18 to 10.53 ± 1.21 Bq/l, respectively. The canal is divided into three zones: before the industrial zone [A], the industrial zone [B] (including the Petroleum Company, the Delta Company for Iron, Aluminium Sulfate Company, the Abou-Zabal (AZ) Company, and sulfate of aluminium and potassium company), and after the industrial zone [C]. The ^{226}Ra, ^{232}Th, and ^{40}K distributions over two seasons were almost identical in zones [A] and

[C], which is compatible with the distribution pattern of the elements in the River Nile (El-Gamal et al. 2019a, b). However, the mean specific activity of ^{226}Ra, ^{232}Th, and ^{40}K in zone [B] (the industrial zone) was more than twice that of zones [A] and [C]. Significant variations in the activity concentrations of ^{226}Ra, ^{232}Th, and ^{40}K were observed in the industrial region, with an increase in the activity concentration of ^{232}Th and ^{40}K during the summer and a rise in ^{226}Ra during the winter. The mean activity concentration of ^{226}Ra decreased with increasing sampling distance from the industrial zone [B], which includes the Abu Za'baal Fertiliser Factory, the Petroleum Company, the Delta Company for iron, and the Aluminium Sulfate Company.

Radium is less common than other alkaline earth metals due to its low natural abundance. It exists as Ra $^{2+}$, which is poorly soluble in natural water (Chu and Wang 2000), often precipitating in sulfate, carbonate, and chromate salts (Edsfeldt 2001). Additionally, Ra-226 decays by alpha particle radiation into radon-222, a gas with a

Table 3 The activity concentration of radionuclides in water samples (Bq/l), sediment samples, commercial fertilizers, and raw materials (Bq/kg) (activity ± total error)

Sample code		Water						Sediment					
		Ra-226 series		Th-232 series		K-40		Ra-226 series		Th-232 series		K-40	
		Winter	Summer	Winter	Summer	Winter	Summer	Winter	Summer	Winter	Summer	Winter	Summer
Before the industrial zone [A]	M1	0.25±0.05	0.35±0.03	0.35±0.11	0.4±0.09	2.66±0.26	2.44±0.18	20.78±0.98	10.18±0.59	28.09±1.63	5.80±0.50	190.56±4.03	150.45±3.27
	M2	0.35±0.09	0.41±0.08	0.21±0.09	0.36±0.08	1.85±0.25	1.67±0.18	25.51±1.60	15.52±0.69	10.87±1.15	18.86±1.62	244.31±6.29	320.45±8.06
The industrial zone [B]	M3	0.60±0.03	0.47±0.09	0.49±0.06	0.42±0.07	3.53±0.05	5.78±0.73	25.12±1.73	29.56±1.41	14.05±1.31	18.28±1.14	296.22±8.54	251.09±5.48
	M4	0.59±0.09	0.46±0.04	0.60±0.14	0.69±0.10	4.77±0.11	2.40±0.19	23.09±1.19	24.93±1.33	14.62±1.02	13.67±1.33	309.12±5.75	182.68±6.22
	M5	0.54±0.10	0.60±0.04	0.29±0.08	0.45±0.06	2.56±0.42	3.56±0.34	28.72±1.26	27.4±1.54	23.20±2.99	12.58±1.16	424.36±16.44	270.20±6.38
	M6	0.93±0.06	1.03±0.14	1.01±0.16	0.94±0.05	6.10±0.56	10.53±1.21	35.13±2.01	30.01±1.67	17.66±1.28	10.55±1.33	332.33±7.48	272.7±6.95
	M7	1.43±0.22	0.88±0.08	0.74±0.13	0.93±0.12	10.68±1.39	10.00±0.83	41.16±0.79	35.45±0.61	14.75±0.99	9.26±0.47	333.32±4.66	257.22±2.72
	M8	0.36±0.07	0.52±0.07	0.61±0.09	0.76±0.11	5.52±0.68	8.69±0.77	61.07±3.56	39.48±1.50	29.63±2.5	17.58±1.16	590.01±13.21	375.96±5.02
	M9	0.47±0.03	0.60±0.05	0.77±0.1	0.59±0.07	3.45±0.3	7.61±0.54	54.15±1.19	41.1±1.17	7.8±0.68	13.28±1.09	363.45±8.80	351.13±7.59
After the industrial zone [C]	M10	0.35±0.04	0.42±0.04	0.48±0.12	0.20±0.04	4.23±0.68	1.91±0.10	25.62±1.14	23.66±0.70	8.75±0.7	11.37±1.05	165.21±3.35	116.97±2.62
	M11	0.3±0.04	0.34±0.05	0.34±0.12	0.19±0.02	4.03±0.65	4.80±0.61	26.82±1.62	19.60±0.94	14.92±1.19	10.78±0.78	281.91±7.42	139.35±3.80
	M12	0.28±0.02	0.3±0.04	0.3±0.12	0.22±0.02	3.39±0.39	2.78±0.41	22.55±2.17	25.62±0.75	11.48±1.16	11.32±0.52	141.04±7.36	203.71±3.26
	M13	0.26±0.02	0.28±0.04	0.26±0.02	0.25±0.06	2.94±0.1	3.45±0.50	14.19±1.21	17.48±0.41	14.66±1.20	13.36±0.78	134.40±5.15	98.48±2.75
Mean (Canal)		0.52±0.07	0.51±0.06	0.50±0.1	0.49±0.07	4.29±0.45	5.05±0.51	31.07±1.57	26.15±1.02	16.19±1.37	12.82±0.99	292.79±7.58	230.02±4.93
Worldwide (WHO 2003; IAEA 1996)	1			1		4		35		35		370	

Phosphate fertilizer samples

Sample code		Ra-226 series	Th-232 series	K-40
Granulated single super phosphate (SSP)	Commercial fertilizers	268.11±2.62	19.48±1.27	241.24±4.28
Phosphorus calcium sulfate (PCS)		99.64±2.06	22.51±1.52	406.66±5.49
R1	Raw materials	362.61±2.53	25.19±1.12	327.04±4.62
R2		390.23±2.91	23.56±1.7	310.21±4.02
Soil sample	Collected 100–150 m from fertilizer company	73.2±2.5	18.51±0.98	350.23±4.98
Control sediment sample (River Nile sample)		26±1.6	19±1.5	205±4.5

high probability of decaying in the body when inhaled, emitting alpha particle radiation in the body. The long-term exposure of people to high concentrations of radon and its progeny in mines and phosphate factories causes pathological effects, including functional changes in the respiratory system and lung cancer (Dajawa et al. 2009). Low values of ^{226}Ra near the Aluminium Sulfate Company at stations M8 and M9 could result from radium precipitation from water due to seepage of sulfate from the Aluminium Sulfate Company. In the same context, the ^{232}Th and ^{40}K have a significant impact with higher activity concentrations in the industrial zone compared to the rest of the canal, especially during the summer. Thorium is particularly insoluble in natural waters and tends to be combined with solid materials (El-Reefy et al. 2010).

Furthermore, thorium is challenging to transfer in any environment due to the strong stability of the insoluble oxide ThO_2 (Mamoney and Khater 2004). Modest seasonal variation in ^{40}K concentrations, rising during the summer (season of agriculture), may be due to dissolved potassium due to the increased water flow. The natural radioactivity of most of the sampling stations of the canal during two seasons falls within the permissible limits of natural radionuclides, except for some stations, such as M6 and M7, exhibiting higher natural radioactivity than the worldwide value of drinking water (IAEA 1996; WHO 2003). This may be due to the accumulation of phosphate dust and phosphorus ore and processing waste discharging into the canal near the canal's shoreline.

Sediment

The specific activity concentration of ^{226}Ra, ^{232}Th, and ^{40}K in sediment was determined in becquerel per kilogram during two seasons, as illustrated in Fig. 2 and Table 3. The activity of radionuclides for ^{226}Ra, ^{232}Th, and ^{40}K varied from 14.19 ± 1.21 Bq/kg at M13 to 60.01 ± 3.56 Bq/kg at M8, 7.8 ± 0.68 Bq/kg at M9 to 29.63 ± 2.5 Bq/kg at M8, and 134.4 ± 5.15 Bq/kg at M13 to 590.01 ± 13.21 Bq/kg at M8, respectively, during the winter. In summer, the range was 10.18 ± 0.59 to 41.1 ± 1.17 Bq/kg, 5.80 ± 0.50 to 18.86 ± 1.62 Bq/kg, and 98.48 ± 2.75 to 375.96 ± 5.02 Bq/kg, respectively. Our findings indicated that the ^{226}Ra concentration in zones [A] and [C] falls within the typical range of unpolluted surface sediments (20–30 Bq/kg) for ^{226}Ra concentration (Bolivar et al. 1996), but the activity concentration of ^{226}Ra was higher three times in the sediments of zone [B]. This enhancement was concentrated noticeably close to the canal discharge locations for the Abu Za'baal Fertilizer & Chemical Company and Aluminium Sulfate

Company. The wastes from processing phosphate and phosphate raw materials uploaded into the canal side from loaders and transported over the road by conveyor belt to the manufacturing area may be the reason for the high ^{226}Ra concentration in this canal area. This is further confirmed by the soil sample taken at a distance of 100–150 m from the fertilizer factory, which contains a high level of radium (Fig. 3).

Moreover, the Ismailia Canal passes through different geologic formations, with sand and marl downstream and silt and mud upstream of the canal (El-Mathana et al. 2021). About 80% of Nile water from the Blue Nile and Atbara rivers originates from highland Ethiopia, mainly mafic and basalt rocks low in naturally occurring radioactive elements (Turekian and Wedepohl 1961). Therefore, the possible explanation for the high amount of ^{226}Ra in the sediment is the impact of the Abu Za'baal Fertilizer & Chemical Company and the Aluminium Sulfate Company.

The precipitated radium from water into sediment may lead to the highest ^{226}Ra concentration in sediment and the lowest ^{226}Ra concentration in the water near the Aluminium Sulfate Company at the station (M8) during winter and at the station (M9) during summer. When highly saturated, radium tends to co-precipitate with sulfate to form radio-barite ($RaSO_4$) rather than supersaturated carbonate minerals (Menzie et al. 2008; IAEA 2014). Over time, as radium with sulfate accumulates in easily carried fine-grained sediments, it mobilizes to locations with lower radioactive element concentrations (Elizabeth and Phillips 2001; Renock et al. 2016). At the same time, Ismailia Canal sediment was dominated by a small grain size (128 μm), possibly due to clay precipitation at the canal bottom (Youssef et al. 2004). Additionally, the Abu Za'baal region showed Oligocene basalt on the surface of the sediment, which is dominated by sands, gravel, and fractured basalt (Kandil et al. 2023).

The ^{232}Th levels in sediment samples revealed minimal values, indicating that the industrial zone had little impact on the distribution of thorium. ^{232}Th activity levels in sediment samples are substantially lower than those of Ra. This might be because the sediment contains Th as a very insoluble oxide, and the bioavailability of thorium is likewise very low, leading to the hypothesis of a common threat of Th-232 in industrial areas. Conversely, a relatively high concentration of ^{40}K was determined in sediment samples in zone [B], more than in zones [A] and [C]. This might occur because one of the company's commercial products (phosphoric calcium sulfate) has high potassium and calcium carbonate levels.

Furthermore, the limestone-based banks of the Nile Valley contribute to the Ca, Na, and HCO_3 enrichment in the Ismailia Canal media (Ramadan et al. 2015).
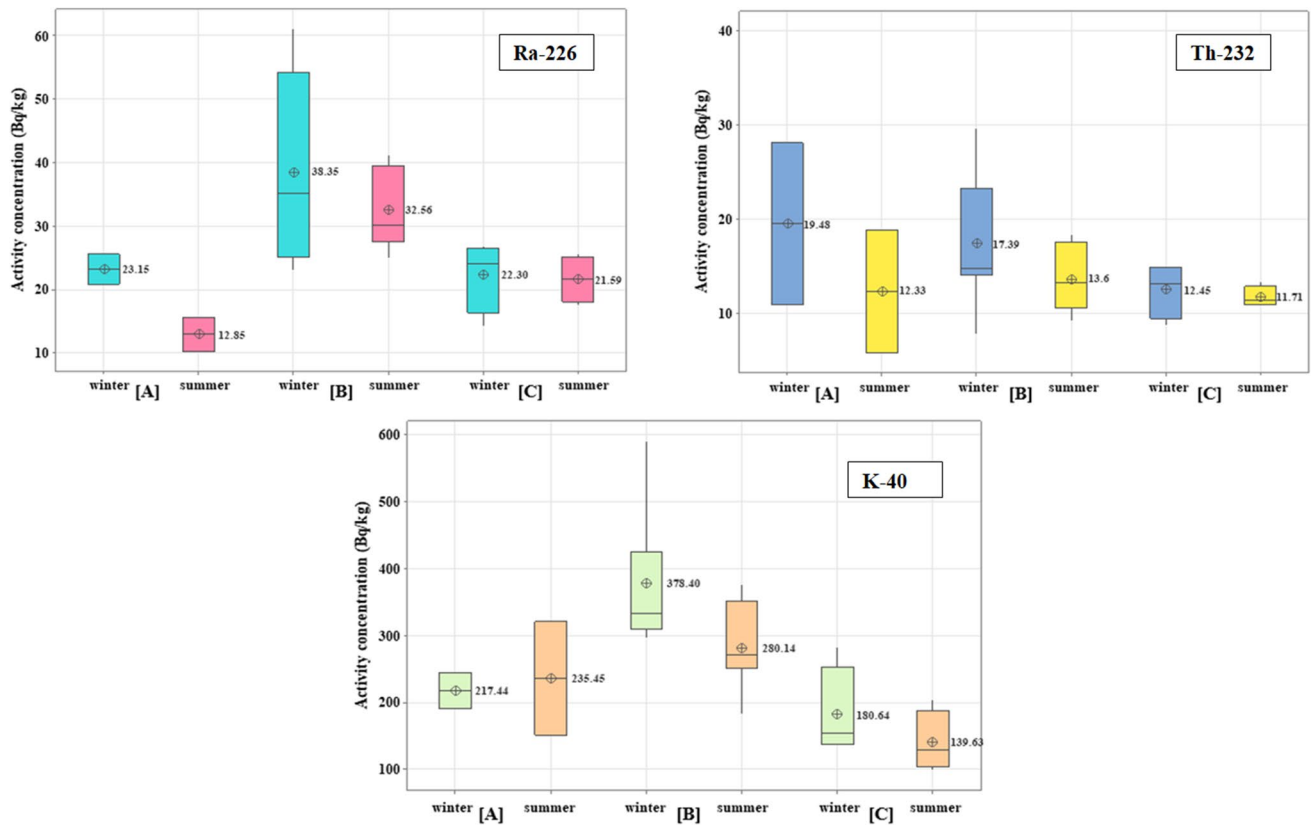
Fig. 3 The distribution of ^{226}Ra-series, ^{232}Th-series, and ^{40}K in sediment samples of Ismailia Canal

Anthropogenic activities cause variations in the concentrations of radionuclides, while others result from natural processes controlled by the mineralogy of the rock or soil. The results showed that the mean activity concentration of ^{226}Ra, ^{232}Th, and ^{40}K in sediment samples during winter is higher than during summer and lower than the worldwide value (UNSCEAR 2000).

Fertilizer samples

The radionuclide activity concentration in the commercial fertilizers and raw materials from Abu Za'baal Fertilizer & Chemical Company is illustrated in Table 3 and Fig. 4. Granulated single super phosphate (SSP) (17% P_2O_5) and phosphorus calcium sulfate (PCS) (0.5% P_2O_5, 6% calcium, and 13% sulfate) are two samples from the local market, in addition to two samples of raw materials. The activity concentrations of ^{226}Ra, ^{232}Th, and ^{40}K for SSP were 268.11 ± 2.62, 19.48 ± 1.27, and 241.24 ± 4.28 Bq/kg, respectively. Likewise, for PCS, it was 99.64 ± 2.06, 22.51 ± 1.52, and 406.66 ± 5.49 Bq/kg, respectively. For the raw materials, the specific activity concentrations

of ^{226}Ra, ^{232}Th, and ^{40}K varied from 362.61 ± 2.53 to 390.23 ± 2.91, 23.56 ± 1.7 to 25.19 ± 1.12, and 310.21 ± 4.02 to 327.04 ± 4.62 Bq/kg, respectively. According to fertilizer investigation findings, raw material samples have higher ^{226}Ra activity concentrations than commercial fertilizers (SSP and PCS). All fertilizer sample ^{232}Th concentrations displayed shallow values. Additionally, a sample of phosphorus calcium sulfate fertilizer with K as its primary component exhibited a relatively high concentration of ^{40}K. Furthermore, in a soil sample taken from a fertilizer company 100 to 150 m away, the activity of the radionuclides ^{226}Ra, ^{232}Th, and ^{40}K was 73.2 ± 2.5, 18.51 ± 0.98, and 350.23 ± 4.98 Bq/kg, respectively. These findings are more significant than those of the control sediment sample and the global average value of ^{226}Ra in soil samples (UNSCEAR 2000). The presence of waste products and the dust from raw materials that settle near the factory is likely responsible for this elevated concentration of ^{226}Ra.

Table 4 compares ^{226}Ra, ^{232}Th, and ^{40}K activity concentrations in water, sediment, and phosphate fertilizer samples from the study area to those previously
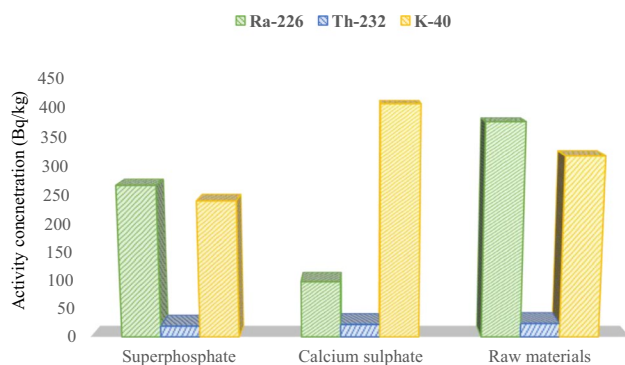
Fig. 4 Comparison between the activity concentration of ^{226}Ra, ^{232}Th, and ^{40}K for the commercial fertilizers (SSP and PCS) and the average value of raw materials

investigated in different countries worldwide. The mean activity concentrations of ^{226}Ra, ^{232}Th, and ^{40}K in the investigated water were consistent with those found in Lake Nasser's freshwater (Imam et al. 2020), and it was lower than those found in the Ismailia Canal (Ramadan et al. 2015). Additionally, the ^{226}Ra activity

concentration was consistent with a water sample from the Nile River close to the Abu-Tartur fertilizer company (Mourad et al. 2009). On the other side, the activity concentration of ^{40}K in this study was higher than those in the Ismailia Canal (Ramadan et al. 2015) and the water sample from the Nile River close to the Abu-Tartur phosphate fertilizer company (Mourad et al. 2009). Similarly, the mean activity concentration of ^{226}Ra in the sediment aligns with those in the Ismailia Canal (Badawy et al. 2015), Lake Nasser (Imam et al. 2020), and the sediment sample from the River Nile next to the Abu-Tartur phosphate fertilizer company (Mourad et al. 2009). Furthermore, the activity concentration of ^{232}Th agrees with the sediment sample from the River Nile next to the Abu-Tartur phosphate fertilizer company (Mourad et al. 2009) and Lake Nasser (Imam et al. 2020). The activity concentration of ^{40}K agreed with Lake Nasser (Imam et al. 2020) and sediment samples from the Nile River close to the Abu-Tartur phosphate fertilizer company (Mourad et al. 2009) and was lower than the Ismailia Canal (Badawy et al. 2015).

Table 4 A comparison of the activity concentrations of ^{226}Ra, ^{232}Th, and ^{40}K in water, sediment samples from the investigation area, and phosphate fertilizer samples from the Abu Za'baal Company with previous studies from different countries

Country	^{226}Ra-series	^{232}Th-series	^{40}K	Note	Reference
Ismailia Canal	0.52 ± 0.07 28.61 ± 1.30	0.50 ± 0.8 14.51 ± 1.18	4.67 ± 0.48 261.41 ± 6.26	Water Sediment	Present study
Ismailia Canal	0.1–2.8	0.1–2.3	0.4–1.2	Water	Ramadan et al. (2015)
Ismailia Canal	24 ± 1.4	21 ± 1.1	323.8 ± 3.41	Sediment	Badawy et al. (2015)
Lake Nasser, Egypt	0.43 ± 0.08 26 ± 1.6	0.44 ± 0.1 19 ± 1.5	4.4 ± 0.93 255.6 ± 7.9	Freshwater Sediment	Imam et al. (2020)
A long the Nile River close to the Abu-Tartur phosphate fertilizer company, Egypt	0.06–1.3 15.4–33.8	0.02–0.16 10.4–19.3	0.14–0.6 128–281	Water Sediment	Mourad et al. (2009)
Abu Za'baal phosphate plant	268.11 ± 2.62	19.48 ± 1.27	241.24 ± 4.28	Granulated single superphosphate (SSP)	Present study
	99.64 ± 2.06	22.51 ± 1.52	406.66 ± 5.49	Phosphorus calcium sulfate (PCS)	
	376.42 ± 2.72	24.38 ± 1.41	318.63 ± 4.32	Raw materials	
Abu Za'baal phosphate plant, Egypt	301 ± 3.9	24 ± 1.4	3 ± 0.9	Superphosphate	Hussein (1994)
Abu-Tartur phosphate company, Egypt	778 ± 27 627 ± 24	12.4 ± 2.8 6.1 ± 2.4	51.6 ± 7.8 8.2 ± 2.2	Phosphate raw Superphosphate	Mourad et al. (2009)
Assuit fertilizer factory, Upper Egypt	445.50 ± 24.38	126.23 ± 6.31	192.22 ± 9.61	Superphosphate	El-Taher and Makhluf (2010)
Fertilizer samples from the Indian markets, India	527 ± 15	7 ± 0.2	87 ± 2.0	Superphosphate	Chauhan et al. (2013)
Brazil	375	100	871	Superphosphate	Saueia et al. (2005)
Saudi Arabia	55.2	8.86	553	Superphosphate	El-Taher and Abdelhalim (2013)
Bangladesh	143	-	292	Superphosphate	Alam et al. (1997)
Pakistan	221	49.7	556	Superphosphate	Khan et al. (1998

Table 4 compares the concentrations of ^{226}Ra, ^{232}Th, and ^{40}K for phosphate fertilizer samples, specifically single super phosphate fertilizer, phosphorus calcium sulfate (PCS), and phosphate raw material worldwide. Regarding ^{226}Ra, the single super phosphate fertilizer agrees with those found in the Abu Za'baal phosphate plant (Hussein 1994) and Pakistan (Khan et al. 1998). Whereas it was higher than that of Saudi Arabia (El-Taher and Abdelhalim 2013) and Bangladesh (Alam et al. 1997), it remained lower than the fertilizer samples from the Indian markets, India (Chauhan et al. 2013); Brazil (Saueia et al. 2005); Assuit fertilizer factory, Upper Egypt (El-Taher and Makhluf 2010); and Abu-Tartur phosphate company, Egypt (Mourad et al. 2009). The activity concentration of ^{232}Th in phosphate fertilizer samples was higher than those found in Bangladesh (Alam et al. 1997); fertilizer samples from the Indian markets, India (Chauhan et al. 2013); Abu-Tartur phosphate company, Egypt (Mourad et al. 2009); and Saudi Arabia (El-Taher and Abdelhalim 2013), and it remained lower than Abu Za'baal phosphate plant (Hussein 1994); Pakistan (Khan et al. 1998); Assuit fertilizer factory, Upper Egypt (El-Taher and Makhluf 2010); and Brazil (Saueia et al. 2005). Moreover, the activity concentration of ^{40}K aligns with the Assuit fertilizer factory, Upper Egypt (El-Taher and Makhluf 2010) and Bangladesh (Alam et al. 1997), yet remains lower than Brazil (Saueia et al. 2005), Pakistan (Khan et al. 1998), and Saudi Arabia (El-Taher and Abdelhalim 2013). Conversely, it is higher than levels found in the Abu Za'baal phosphate plant (Hussein 1994), Abu-Tartur phosphate company, Egypt (Mourad et al. 2009), and fertilizer samples from the Indian markets, India (Chauhan et al. 2013). Regarding raw materials, the activity concentration of ^{226}Ra was lower than that of Abu-Tartur phosphate company, Egypt (Mourad et al. 2009), while ^{232}Th and ^{40}K were higher than those reported for Abu-Tartur phosphate company, Egypt (Mourad et al. 2009).

Diatom community composition

A total of 84 species belonging to 12 orders (Achnanthales, Aulacoseirales, Bacillariales, Cymbellales, Eunotiales, Fragilariales, Naviculales, Rhabdonematales, Rhopalodiales, Surirellales, Thalassiophysales, and Thalassiosirales) and 23 genera were recorded over the investigated period (Rhabdonematales and Surirellales were recorded only in winter). Based on the number of species, the wealthiest two orders were Bacillariales (including 15 species across four genera, with the genus Nitzschia comprising 12 species) and Naviculales (including 15 species across three genera, with the genus Navicula comprising 13 species), followed by the order Cymbellales, encompassing ten species belonging to two genera *Cymbella* and *Gomphonema*.

The comparison did not display an evident seasonal variation (ANOVA, P-value = 0.15) in diatom abundance from winter to summer (Sherwood et al. 2000). This was evident in non-taxonomic attributes. However, the variability was evident among the sampling sites, potentially explaining changes in water trophic and ecological conditions. The spatial and temporal diatom distribution is represented in Fig. 5. The distribution of diatoms recorded in winter showed the highest density at sites (3) and (1), with abundances of 4×10^7 cells/cm^3 and 3×10^7 cells/cm^3, respectively. In summer, the highest density was recorded at site 11, followed by site 10 with 18.6×10^6 cells/cm^3 and 11×10^6 cells/cm^3, respectively. Diatom genera *Cyclotell*, *Fragillaria*, and *Aulacoseira* dominate the winter and summer peaks.

On the other hand, the lowest densities in winter were recorded at sites (6) (fertilizer Company), (4) (Petroleum Company drain), and (8) (Aluminium Sulfate Company drain), with 1×10^6 cells/cm^3 and 2×10^6 cells/cm^3, respectively. In summer, the least density was recorded at sites (4) and (1), with 0.12×10^6 cells/cm^3 and 0.32×10^6 cells/cm^3, respectively (Fig. 5). The spatial diatom densities were accompanied by the presence or absence of industrial activity. The highest densities were recorded at either zone [A] as in site one during winter (26.5×10^6 cells/cm^3) or [C] in site 10 (12.03×10^6 cells/cm^3 and 10.9×10^6 cells/cm^3 in winter and summer, respectively) and 11 (11.6×10^6 cells/cm^3 and 18.6×10^6 cells/cm^3 in winter and summer, respectively). Conversely, the lowest densities were recorded in zone [B], which included the industrial activities in the studied area of the canal, except at site 3 in winter, where the highest density of all parameters is still in the same range of zone [A]. The diatom community's health, distribution, and the presence or absence of tolerant and sensitive species are significantly affected by the fertilizer company's drain, leading to high phosphate and raw phosphate material waste. Besides the species of common occurrence (e.g., *Cyclotella ocellata*), samples collected at the fertilizer Company drain revealed a considerable density of tolerant and eutrophic species, *Nitzschia palea* (van Dam et al. 1994). *Nitzschia palea* is commonly associated with urban sites and areas polluted by residential and industrial effluents (Ndiritu et al. 2006). Generally, small species dominate stressful environments due to their fast metabolism (Falasco et al. 2009); however, large species are sensitive to stressful conditions. Additionally, some species may be more resistant to this radioactive stress than others.

Fig. 5 Spatial and temporal variations of diatom densities (individuals/cm$^3 \times 10^{-6}$) at sites of Ismailia Canal during two seasons
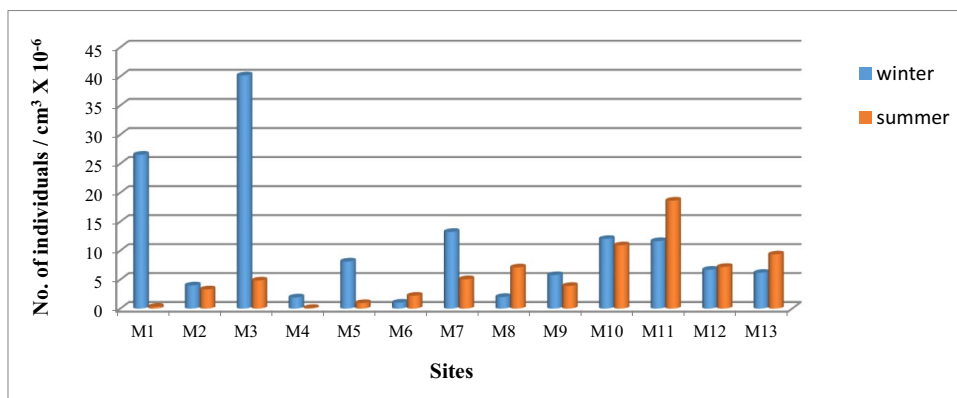
Influence of physicochemical and radioactive elements on diatom diversity, richness, and evenness

In terms of Shannon's diversity index, the lowest diversity was recorded at sites (12) and (13), while the highest diversity occurred at sites (10) and (2) during winter and summer, respectively. Despite the high richness in diatom composition at each site, most sites were dominated by *Aulacoseira*, *Cyclotella*, and *Fragilaria* species without abnormalities. It is predicted that diversity, richness, and evenness will decline with increased human disturbance of habitats, leading to locations dominated by cosmopolitan species (*Aulacoseira*, *Cyclotella*, and *Fragilaria*), which are prevalent in most regions in the River Nile in Egypt. Richness during the winter ranged from 0.56 at the poorest site (2) to 1.64 at the highest site (10). In the summer, it ranged from 0.6 at the richest site (4) to 1.8 at the richest site (7). The highest abundance and dominance of *Aulacoseira granulata* at a site (1) in winter indicate the least evenness. Conversely, sites (12) and (13) represent the lowest evenness value in summer due to the high abundance of *Cyclotella ocellata* and *Fragilaria construens* species, constituting more than 85% of total diatom abundance. The correlation between diatom diversity, richness, evenness, and physico-chemical and radionuclides is presented in Table 5. Significant correlations ($P < 0.05$) were observed between diatom richness, diversity, evenness, and some physicochemical or radionuclide elements. Evenness was positively correlated with temperature in summer, EC, magnesium, R-226, and K-40. These conditions are not preferable for specific species, so the dominance was distributed fairly.

Relationships between environmental variables, radionuclides, and biological community

Environmental variables, major elements, and radionuclide analysis

The findings of the multivariate redundancy analysis (RDA) for environmental factors, nutrient salts, significant elements, and radioactive elements in the water and sediment are shown in Fig. 6 A and B, respectively. In water, the RDA results for environmental variables, nutrient salts, and major elements with radionuclides for the first two axes accounted for 98.3% of the total variance, with the first two principal components (F1 = 92.9%, F2 = 5.4%). The analysis demonstrated a significant correlation between parameters (pH, Na, TDS, PO$_4$, SO$_4$, SiO$_2$, K, and CO$_3$) and radionuclides (Ra-226, Th-232, and K-40). A moderate positive correlation was observed between ^{226}Ra and TDS, pH, PO$_4$, Na, SiO$_2$, and SO$_4$ ($r > 0.5$), indicating the precipitation of Ra-226 as soluble salts in the canal due to sulfate, as confirmed by Edsfeldt (2001). Correlations between Ra-226 and phosphorus and silicon dioxide at stations (M6) and (M7) further support the influence of the Aluminium Sulfate Company and Abu Za'baal Fertilizer and Chemical Companies. Statistical analysis revealed that the radioactivity elements ^{226}Ra, ^{232}Th, and ^{40}K were linked with the high radioactive materials source. A negative correlation was also observed between Ra-226 and K (stable potassium) and CO$_3$ (carbonate). Furthermore, a moderate positive correlation was noted between ^{40}K and pH and CO$_3$.

Likewise, the RDA results for radionuclides and environmental variables, nutrient salts, and major elements in the sediment showed that axes 1 and 2 accounted for 77.1%

Table 5 Pearson correlation coefficient (*r*) between diatom (richness, evenness, diversity) and the physicochemical and radioactive elements measured in Ismailia Canal; Temp, temperature; E.C, electrical conductivity; BOD, biological oxygen demand; TP, total phosphorous. Ra-226, Th-232, and K-40 represent radionuclides activity during winter (w) and summer (S)

| Diatom	Seasons	Temp °C	EC µS/cm	pH	BOD mg/l	NH_4^+ µg/l	SiO_2 mg/l	TP µg/l	Na mg/l	K mg/l	Mg mg/l	Ca mg/l	Ra-226 Bq/kg	Th-232 Bq/kg	K-40 Bq/kg
Richness	W	0.098	−0.446	0.077	0.196	**0.544**	−0.115	−0.131	−0.462	0.134	**−0.650**	0.330	−0.377	0.111	−0.312
	S	**−0.550**	−0.115	0.419	**−0.580**	−0.415	−0.055	−0.016	0.015	0.179	**0.549**	**−0.740**	0.123	0.262	0.242
Evenness	W	−0.013	**0.689**	−0.210	−0.237	**−0.558**	0.160	0.027	0.439	−0.057	**0.630**	−0.322	**0.624**	0.117	**0.551**
	S	**0.745**	0.126	−0.073	0.095	0.293	0.348	−0.134	−0.139	−0.281	**−0.533**	0.317	−0.092	−0.131	0.176
Diversity	W	0.117	0.256	0.073	−0.024	0.118	−0.024	−0.233	−0.025	0.072	−0.070	0.058	0.396	0.264	0.388
	S	0.236	0.131	0.296	−0.332	−0.109	0.307	−0.047	−0.127	−0.104	−0.064	−0.203	0.045	0.051	0.423

The bold emphasis represented the significance correlation

and 17.9% of the total variation, respectively (Fig. 6B). The analysis indicated that the correlation between the parameters and elements behaves differently in sediment. Significant correlations were found between radionuclides and DO, HCO_3, COD, TDS, SO_4, Na, Mg, pH, TP, and CO_3. This may reflect the relationship between the mineral dolomite ($CaMg(CO_3)_2$) found in the limestone and the presence of radionuclides (i.e., uranium and thorium series) in the limestone, consistent with previous findings (Kim 1995). A moderate positive correlation was also detected between Ra-226 and TDS, Na, and COD. These analyses show a statistically significant correlation between the physicochemical parameters (pH, TDS, and DO) and 226Ra, confirming that the behaviour of the radiation emitted by the different radionuclides depends on the overlying soil materials, the chelating agents, the physicochemical properties, and the type of rock (Belivermis et al. 2010). The correlation between COD and Ra-226 and K-40 suggests that more oxygen is needed to oxidize, indicating the possibility of additional oxidation (Camacho et al. 2012). Furthermore, there was a positive correlation between TP and K-40 and a weakly negative correlation with Ra-226 and Th-232.

Taxonomic characteristics of diatoms with the tested variables

The multivariate redundancy analysis (RDA) of the ecological conditions showed that the non-impacted sites were significantly different from the impacted sites, indicating that the discharge of industrial effluents caused a modification of the physicochemical characteristics of the canal water, inducing enrichment of Ra-226, Th-232, and K-40, major cations (Ca^{++}, Mg^{++}, K^+, and Na^+), sulfate, total phosphorus, ammonium, and silicate. RDA analysis was also performed to test the effect of physical, chemical, and radionuclide elements on the diatom data (Fig. 6C). The analysis included species with a frequency of $\geq 30\%$ (Table 6). Species-environment correlations were 0.9 and 0.8 with the first and second axes, respectively. The variance explained by all tested variables was 0.86 ($P = 0.002$), of which 0.21 was presented by Mg ($r = 0.6$, $P = 0.004$) and 0.15 was defined by the activity concentration of ^{226}Ra, ^{232}Th, and ^{40}K ($r = -0.2$, 0.2, and 0.3, respectively). These findings confirmed that radioactivity threatens the diatom community composition (Millan et al. 2020). The accumulation of these radionuclides in the environment stresses the algae in different ways, including their effect on photosynthesis, chlorophyll production, and the functioning of enzymes (Banerjee et al. 2022).

Generally, under the effect of high-intensity radiation, the microalgae do not grow. However, if a specific type of microorganism has evolved under high-energy radiation, it can overcome the physiological stress in the harsh environment for growth and grow normally (Sukla et al. 2019). The
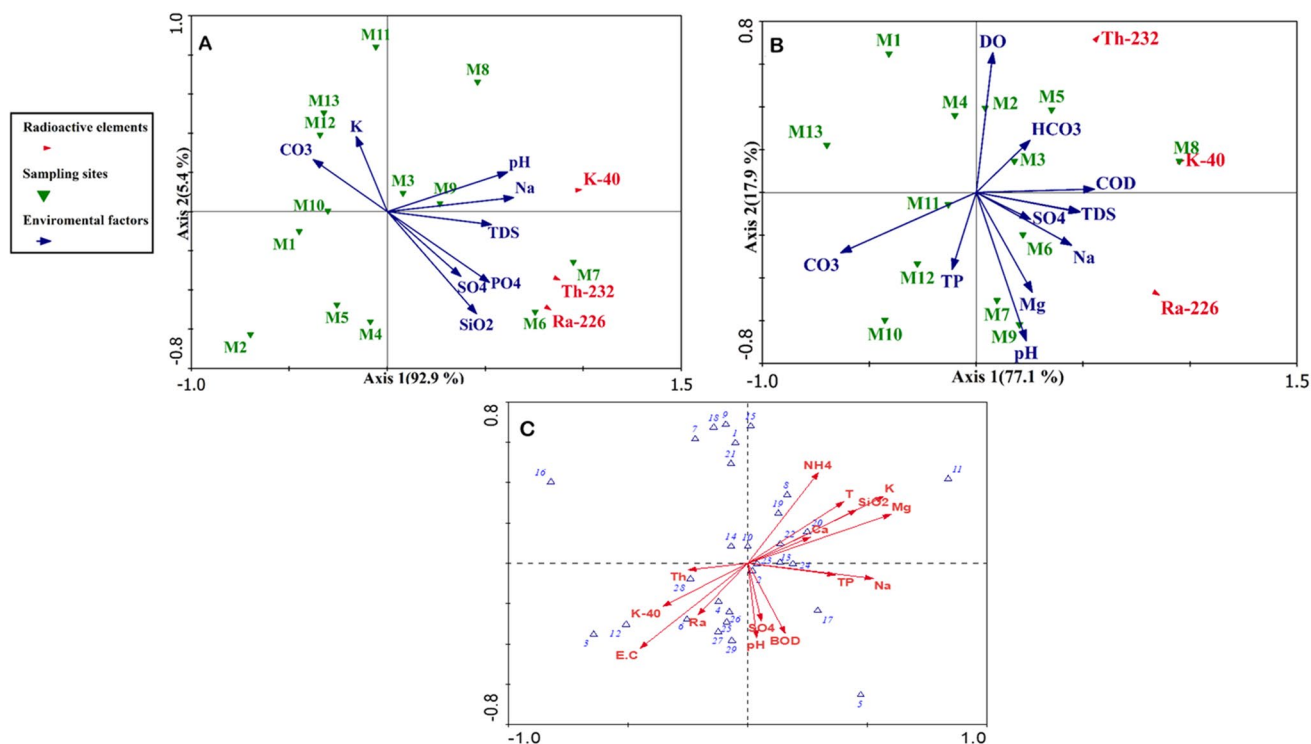
Fig. 6 **A** Redundancy analysis (RDA) biplot of radioactive elements, environmental variables, nutrients, and major cations in water. **B** RDA of radioactive elements, environmental variables, nutrients, and major cations in sediment. **C** RDA of frequently recorded diatom taxa and water conditions (ammonium, NH₄; carbonate, CO₃; bicarbonate,

HCO₃; silicate, SiO₃; sulfate, SO₄ biological oxygen demand, BOD; pH; total phosphorus, TP; phosphate, PO₄; electrical conductivity, E.C; Ra-226 series, Ra; Th-232 series, Th; and K-40 series, K) of Ismailia Canal

impacted radioactive sites support a variety of algae species. Taxa such as *Cyclotella meneghiniana*, *Cymbella affinis*, *Nitzschia frustulum*, *Nitzschia liebetruthii*, *Nitzschia palea*, and *Synedra tenera* are associated with Ra-226 concentration. At the same time, *Cyclotella glomerata* and *Fragilaria ulna* are associated with naturally radioactive K-40, while *Nitzschia paleacea* is associated with a high Th-232 concentration. This association may involve the bioaccumulation of these radionuclides in diatom cells (Heidari et al. 2017) or their uptake for their metabolism. So, in our study, radionuclides do not eliminate diatom species, but some species show associations with radionuclide concentrations.

The major element (Na, K) positively correlated ($r = 0.5$) with the species' first axis. As limiting factors affecting diatom community composition, total phosphorous (TP) and silicate (SiO_2) seemed to explain some of the variance in the diatom community with a correlation matrix of 0.4. Species like *Navicula diluviana* and *Nitzschia dissipata* are associated with TP and SiO_2 concentrations. *Navicula diluviana* has previously been classified as an indicator of TP (Van Dam et al. 1994; Belal

2012). NH₄ is commonly considered one of the principal factors explaining the variation of diatom taxa and a growth-limiting factor (Enache and Prairie 2002). According to RDA (Fig. 8), NH₄ can be considered a common factor in explaining the variability of the diatom communities with a correlation matrix of 0.3. *Epithemia sorex* and *Navicula digitoradiata* are correlated species, suggesting that these species can live in a wide range of ammonium concentrations (Belal 2012). While phosphorus and nitrogen are essential growth-promoting factors, their high concentrations, especially in agricultural areas, can affect diatom diversity, as seen in some affected sites. Meanwhile, the variance of the diatom community structure was slightly explained by pH and SO₄, which did not significantly contribute to our understanding of the community structure of the diatoms found in the water of the Ismailia Canal. A group of commonly distributed species (*Achnanthidium minutissimum*, *Cymbella microcephala*, *Eunotia* sp., *Gomphonema parvulum*, *Navicula anglica* var. *subsalsa*, and *Navicula pupula*) was categorized, indicating a slight effect of most studied variables (Belal 2012).

Table 6 Seasonal average of relative abundance of most frequent (≥30%) attached diatom taxa identified from Ismailia Canal

RDA code	Species name	Currently accepted nomenclature	M1	M2	M3	M4	M5	M6	M7	M8	M9	M10	M11	M12	M13
1	*Achnanthidium minutissimum* (Kützing) Czarnecki		1.93	0	0.11	0.27	0.36	0	0.38	1.1	0	0.44	0.62	0.38	0.77
2	*Cocconeis placentula* Ehrenberg		0.95	0.33	0.17	4.68	0.43	1.16	0.3	0.39	0.14	0.25	0.66	0.4	0.89
3	*Cyclotella glomerata* H. Bachmann	*Lindavia glomerata* (H. Bachmann) Adesalu & Julius	8.36	10.9	13	12.2	7.52	9.48	14.3	15.9	10.4	6.83	12	5.22	3.69
4	*Cyclotella meneghiniana* Kützing	*Stephanocyclus meneghinianus* (Kützing) Kulikovskiy, Genkal & Kociolek	0.46	2.6	1.62	2.54	0.14	2.57	1.08	2.98	2.27	1.93	1.66	0.81	0.38
5	*Cyclotella ocellata* Pantocsek	*Pantocsekiella ocellata* (Pantocsek) K. T. Kiss & Ács	23.9	41.4	41.9	48	53.3	51.4	41.6	36.1	45.1	52.8	45.9	49.9	48.5
6	*Cymbella affinis* Kützing		0.04	0.17	0	0.4	0.27	0	0	0.08	0.19	0.09	0.05	0	0
7	*Cymbella microcephala* Grunow	*Encyonopsis microcephala* (Grunow) Krammer	0.9	0	0.14	0	0	0	0.08	0	0.19	0.05	0.08	0	0.18
8	*Epithemia sorex* Kützing		0.08	0.17	0.11	0	0	0	0.05	0.23	0.14	0	0	0	0.06
9	*Eunotia* sp.		0.95	0.17	0.36	0.13	0	0	0.05	0.08	0.47	0.2	0.46	0.24	0.18
10	*Fragilaria biceps* Ehrenberg		0	0.17	0.11	0.13	0	0	0	0.08	0.14	0	0.03	0	0
11	*Fragilaria construens* (Ehrenberg) Grunow	*Staurosira construens* Ehrenberg	14.2	11.7	10	3.48	16.2	17.2	17	21.1	14.7	15.2	23.2	36	38.3
12	*Fragilaria ulna* (Nitzsch) Lange-Bertalot	*Ulnaria ulna* (Nitzsch) Compère	2.11	2.38	1.13	3.74	1.99	0.91	2.59	0.78	1.62	1.48	4.66	0.41	0.33
13	*Fragilaria ulna* var. *acus* (Kützing) Lange-Bertalot	*Ulnaria acus* (Kützing) Aboal	0.04	0	0.17	0	0.36	0.37	0.22	0	0.33	0.09	0.27	0.16	0
14	*Gomphonema minutum* (C. Agardh) C. Agardh		0.04	0.17	0.11	0	0	0	0.05	0.63	0	0.09	0.14	0.16	0.09
15	*Gomphonema parvulum* (Kützing) Kützing		0.86	0	0	0	0	0	0	0.39	0.05	0.05	0.15	0.15	0.06
16	*Melosira granulata* (Ehrenberg) Ralfs	*Aulacoseira granulata* (Ehrenberg) Simonsen	40.9	23.1	23.8	17.8	15.9	7.95	10.2	13.6	20.4	8.5	8.66	3.79	3.04
17	*Melosira granulata* var. *angustissima* O. Müller	*Aulacoseira granulata* var. *angustissima* (O. Müller) Simonsen	0	0.83	0.11	0	0.43	1.82	0.51	0.47	1.18	0.96	0.37	0.15	0.18
18	*Navicula anglica* var. *subsalsa* (Grunow) Cleve	*Hippodonta subsalsa* (Grunow) Pomazkina & Radionova	0.95	0.33	0.14	0	0	0	0.05	0.08	0	0.14	0.06	0.08	0
19	*Navicula digitoradiata* (W. Gregory) Ralfs		0.08	0.17	0.03	0	0	0	0.05	0	0	0	0.09	0.08	0.06
20	*Navicula diluviana* Krasske	*Cymbellafalsa diluviana* (Krasske) Lange-Bertalot & Metzeltin	0	0	0.11	0	0	0	0.38	0	0.28	0	0	0.23	0
21	*Navicula pupula* Kützing	*Sellaphora pupula* (Kützing) Mereschkovsky	0.86	0.17	0	0	0	0.12	0.87	0	0	0	0	0	0
22	*Navicula salinarum* Grunow		0	0.17	0	0	0	0	0.31	0.08	0	0	0.06	0	0
23	*Navicula viridula* (Kützing) Ehrenberg		0.12	0	0	0.27	0	0	1.57	0	0.14	0.23	0.09	0	0.06
24	*Nitzschia dissipata* (Kützing) Rabenhorst		0	0	0.25	0	0	0.12	0	0.08	0	0.09	0.03	0.08	0
25	*Nitzschia frustulum* (Kützing) Grunow		0.08	1.1	0.41	0	0.87	0.37	0.6	0	0	2.75	0.06	0	0
26	*Nitzschia liebetruthii* Rabenhorst		0	1	0	0.4	0.27	0	2.67	0.08	0	0.79	0	0	0.06
27	*Nitzschia palea* (Kützing) W. Smith		0.25	0.72	1.37	2.41	0.83	3.85	1.18	0.08	1.38	0.43	0.06	0	0.3
28	*Nitzschia paleacea* (Grunow) Grunow		0.04	0.33	0.52	0.13	0.07	0.54	0.93	2.75	0	0	0	0	0
29	*Synedra tenera* W. Smith	*Fragilaria tenera* (W. Smith) Lange-Bertalot	0.04	0	0	0	0.14	0	0.17	0	0	0.37	0.05	0	0

Water quality and radiological hazard indices

Water quality index

The values of WQI of Ismailia Canal are presented in Table 7 and illustrated in Fig. 7. Based on the WQI results, canal water can be considered an excellent source of drinking water, aquatic life, and irrigation with WQI 88–97, 97–99, and 96–99, respectively. Moreover, CWQI showed that Ismailia Canal water is suitable for drinking water, irrigation, and aquatic life use, consistent with El Sayed et al. (2023) findings.

Radiation hazard indices

Tables 8 and 9 present the most popular radiological hazard index in water and sediment through two seasons. The cancer risks caused by consuming radium isotopes found in water samples (^{226}Ra and ^{228}Ra) that ranged from $36.14 \pm 2.78 \times 10^{-5}$ to $137.45 \pm 18.57 \times 10^{-5}$ with an average value of $69.69 \pm 12.97 \times 10^{-5}$ in winter and from $31.91 \pm 3.88 \times 10^{-5}$ to $133.95 \pm 10.25 \times 10^{-5}$ with an average value of $69.16 \pm 9.23 \times 10^{-5}$ in summer, as represented in Table 8. The mean cancer risk values were within the acceptable range according to the USEPA (2000) standards, as represented in Fig. 8a. Effective doses were calculated for different age groups, including infants, children, and adults, considering the consumption of ^{226}Ra, ^{232}Th, and ^{40}K in water samples during two seasons. The mean annual effective radiation dose for infants and children from drinking water in the study area is below the permissible effective dose limits set by the WHO

Table 7 WQI and its categorizations of the Ismailia Canal at area under investigation for drinking, irrigation, and aquatic life utilizations

Stations	Drinking water		Irrigation		Aquatic life	
	CWQI	Rank	CWQI	Rank	CWQI	Rank
1	97	Excellent	99	Excellent	98	Excellent
2	95	Good	98	Excellent	97	Excellent
3	97	Excellent	99	Excellent	98	Excellent
4	94	Good	98	Excellent	97	Excellent
5	97	Excellent	99	Excellent	98	Excellent
6	90	Good	97	Excellent	97	Excellent
7	97	Excellent	98	Excellent	98	Excellent
8	88	Good	97	Excellent	96	Excellent
9	97	Excellent	99	Excellent	97	Excellent
10	97	Excellent	99	Excellent	98	Excellent
11	97	Excellent	99	Excellent	99	Excellent
12	97	Excellent	99	Excellent	99	Excellent
13	97	Excellent	99	Excellent	98	Excellent

Fig. 7 WQI of the Ismailia Canal at area under investigation for drinking, irrigation, and aquatic life utilizations
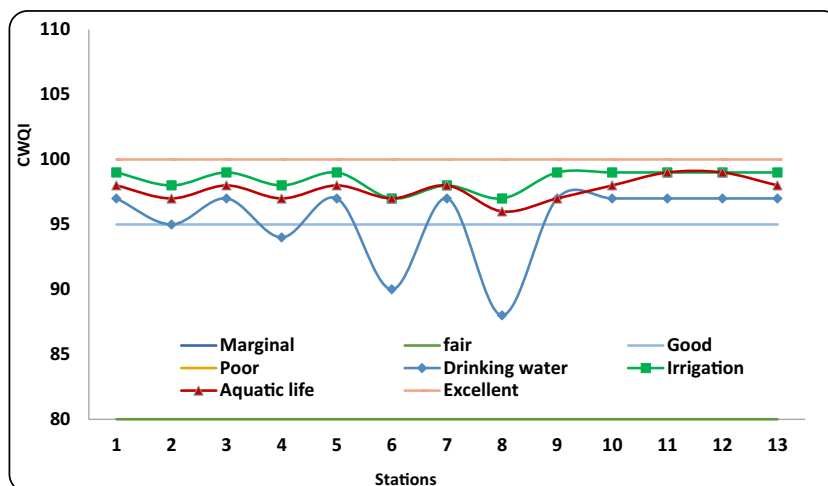
Table 8 The annual effective doses and cancer risk associated with water consumption

Sample no	Cancer risk (CR)×10⁻⁵		Total dose (mSv/year)					
	Winter	Summer	Winter			Summer		
			Infants	Children	Adults	Infants	Children	Adults
M1	44.95±13.09	53.76±10.31	0.09±0.02	0.15±0.03	0.12±0.03	0.09±0.01	0.15±0.02	0.15±0.02
M2	34.32±12.51	51.87±11.12	0.08±0.02	0.14±0.03	0.14±0.03	0.09±0.02	0.16±0.03	0.15±0.03
M3	72.14±7.24	60.21±10.46	0.12±0.01	0.20±0.01	0.17±0.02	0.13±0.02	0.2±0.04	0.19±0.03
M4	83.03±17.62	87.47±11.70	0.14±0.02	0.21±0.04	0.22±0.04	0.13±0.01	0.21±0.02	0.22±0.03
M5	49.48±11.85	68.05±7.61	0.12±0.02	0.21±0.04	0.22±0.04	0.14±0.01	0.23±0.02	0.21±0.02
M6	137.45±18.57	133.95±10.25	0.25±0.02	0.42±0.04	0.27±0.04	0.28±0.03	0.43±0.05	0.42±0.04
M7	128.16±21.37	127.43±15.21	0.24±0.04	0.37±0.08	0.51±0.07	0.25±0.02	0.39±0.04	0.38±0.04
M8	75.61±11.78	96.83±13.82	0.15±0.02	0.23±0.03	0.22±0.03	0.18±0.02	0.26±0.03	0.27±0.04
M9	96.02±11.33	82.37±9.00	0.16±0.01	0.26±0.02	0.21±0.02	0.17±0.02	0.26±0.02	0.26±0.02
M10	61.95±13.74	35.87±5.56	0.12±0.02	0.19±0.03	0.22±0.03	0.09±0.01	0.15±0.02	0.13±0.02
M11	45.79±13.74	31.91±3.88	0.1±0.01	0.15±0.03	0.16±0.03	0.09±0.01	0.14±0.02	0.12±0.02
M12	40.96±13.01	33.51±3.51	0.08±0.01	0.13±0.02	0.13±0.03	0.08±0.01	0.12±0.02	0.11±0.01
M13	36.14±2.78	35.85±7.61	0.08±0.004	0.12±0.01	0.12±0.01	0.08±0.01	0.12±0.02	0.11±0.02
Mean	69.69±12.97	69.16±9.23	0.13±0.01	0.21±0.02	0.21±0.03	0.14±0.02	0.22±0.03	0.21±0.03
Worldwide (WHO 2003; IAEA 1996)[a] (USEPA 2000)[b]	10–100[b]		0.26[a]	0.2[a]	0.1[a]	0.26[a]	0.2[a]	0.1[a]

in 2003. However, the mean annual effective doses of radiation for adults are higher than reference levels, as shown in Fig. 8b. The sites (M6) and (M7) near and downstream of the Abu Za'baal fertilizer company exhibited the highest cancer risk values and effective doses for various age groups in both seasons. In the same context, the mean absorbed dose rate of sediment during the winter and summer is 36.58 ± 1.90 and 29.55 ± 1.31 nGy/h, respectively, which is almost below the reference values provided in UNSCEAR (2000) Report 57 (18–93) nGy/h. In winter, the calculated values of Ra_{eq} ranged from 44.56 ± 3.29 to 144.74 ± 8.06 Bq/kg with an average of 74.72 ± 4.06 Bq/kg, while in summer, they varied from 29.01 ± 1.53 to 90.94 ± 3.51 with an average of 60.59 ± 2.79 Bq/kg. The annual effective dose for sediment samples varied from 0.026 ± 0.002 to 0.087 ± 0.005 mSv/year and between 0.018 ± 0.001 and 0.055 ± 0.002 mSv/year during winter and summer, respectively. Nevertheless, these values are lower than the worldwide limit (0.5 mSv/year) (UNSCEAR 2000) recommended. For sediment samples, the computed external hazard index fluctuated between 0.123 ± 0.009 and 0.402 ± 0.022 with an average of 0.207 ± 0.011 and from 0.081 ± 0.004 to 0.253 ± 0.010 with an average of 0.168 ± 0.008 during winter and summer, respectively. The mean external hazard is lower than the recommended maximum value, suggesting that the investigation area's sediments are acceptable for use as building materials. The representative level index ($I\gamma$) fluctuated between 0.331 ± 0.024 Bq/kg and 1.097 ± 0.058 Bq/kg and from 0.226 ± 0.011 Bq/kg to 0.690 ± 0.025 Bq/kg during winter and summer, respectively. For the reasons mentioned, the representative level index ($I\gamma$) was higher than the worldwide reference value at (M8) during the winter. These results indicated that the mean $I\gamma$ values are less than the accepted recommended values (UNSCEAR 2000). Our findings revealed that the radium equivalent activities (Ra_{eq}), the outdoor annual effective dose (E_{eff}), the external hazard index (H_{ex}), and the representative level index ($I\gamma$) in consideration of the existence of natural radionuclides (^{226}Ra, ^{232}Th, and ^{40}K) remain below the recommended maximum levels of UNSCEAR (2000) during both seasons.

The radiological hazard index of phosphate fertilizer samples is represented in Table 9. The absorbed dose rates for fertilizer samples varied from 74.93 to 190.57 nGy/h, surpassing the worldwide values stated in UNSCEAR 2000. The Ra_{eq} content in fertilizer samples fluctuated between 160.29 and 433.59 Bq/kg, with higher values observed in raw materials. Except for the raw materials, the annual effective dose and the external hazard for the fertilizer samples were less than the worldwide range. The representative level index ($I\gamma$) fluctuated between 1.16 and 2.97 Bq/kg, higher than the recommended maximum levels of UNSCEAR (2000).

Conclusion

The Ismailia Canal serves as a crucial source of drinking water for society and contains valuable fisheries. The primary contributors to pollution in the Ismailia Canal are the

Table 9 The radiological hazard parameters in sediment samples during two seasons and phosphate fertilizer samples

Sample code	D (nGy/h)		Ra$_{eq}$ (Bq/kg)		E$_{eff}$ (mSv/year)		H$_{ex}$		Iγ (Bq/kg)	
	Winter	Summer	Winter	Summer	Winter	Summer	Winter	Summer	Winter	Summer
M1	35.66±1.67	14.66±0.72	74.29±3.59	29.01±1.53	0.044±0.002	0.018±0.001	0.204±0.010	0.081±0.004	0.546±0.026	0.226±0.011
M2	28.59±1.71	32.89±1.71	58.16±3.68	64.92±3.57	0.035±0.002	0.040±0.002	0.162±0.010	0.181±0.010	0.442±0.026	0.506±0.026
M3	32.76±1.97	35.52±1.59	65.95±4.20	73.28±3.42	0.040±0.002	0.044±0.002	0.184±0.012	0.203±0.009	0.505±0.030	0.547±0.024
M4	32.83±1.43	27.55±1.72	65.64±3.05	57.27±3.67	0.040±0.002	0.034±0.002	0.183±0.008	0.158±0.010	0.506±0.022	0.425±0.026
M5	45.87±3.22	31.65±1.70	91.60±6.69	64.30±3.65	0.056±0.004	0.039±0.002	0.255±0.018	0.179±0.010	0.706±0.049	0.489±0.026
M6	40.98±2.03	31.52±1.89	83.65±4.36	64.19±4.06	0.050±0.002	0.039±0.002	0.232±0.012	0.179±0.011	0.632±0.031	0.487±0.029
M7	41.67±1.19	32.33±0.69	85.58±2.53	66.70±1.47	0.051±0.001	0.040±0.001	0.237±0.007	0.185±0.004	0.644±0.018	0.500±0.011
M8	71.06±3.74	44.66±1.62	144.74±8.06	90.94±3.51	0.087±0.005	0.055±0.002	0.402±0.022	0.253±0.010	1.097±0.058	0.690±0.025
M9	43.91±1.34	41.44±1.55	90.75±2.78	84.67±3.26	0.054±0.002	0.051±0.002	0.252±0.008	0.235±0.009	0.681±0.021	0.641±0.024
M10	23.84±1.09	22.66±1.11	49.70±2.38	48.11±2.38	0.029±0.001	0.028±0.001	0.137±0.006	0.132±0.006	0.368±0.017	0.349±0.017
M11	33.45±1.80	21.50±1.08	67.89±3.84	44.77±2.32	0.041±0.002	0.026±0.001	0.189±0.011	0.124±0.006	0.516±0.028	0.331±0.017
M12	23.29±2.01	27.19±0.80	48.84±4.34	56.07±1.72	0.029±0.002	0.033±0.001	0.135±0.012	0.155±0.005	0.359±0.031	0.420±0.012
M13	21.54±1.53	20.54±0.81	44.56±3.29	43.48±1.72	0.026±0.002	0.025±0.001	0.123±0.009	0.119±0.005	0.331±0.024	0.316±0.012
Mean (Canal)	36.58±1.90	29.55±1.31	74.72±4.06	60.59±2.79	0.04±0.001	0.036±0.002	0.207±0.011	0.168±0.008	0.564±0.029	0.456±0.020
Granulated single super phosphate (SSP)	137.75±2.14		312.85±4.7		0.17±0.003		0.85±0.01		2.14±0.03	
Phosphorus calcium sulfate (PCS)	74.93±2.12		160.29±4.6		0.09±0.003		0.44±0.01		1.16±0.03	
Raw materials	190.57±2.28		433.59±5.04		0.23±0.003		1.18±0.01		2.97±0.04	
Worldwide (UNSCEAR 2000) soil	57		<370		0.5		1		1	

Fig. 8 **a** The cancer risk associated due to the consumption of water samples and **b** the annual effective doses associated due to the consumption of water samples

(a)

(b)

- Ismailia Canal winter ■ Ismailia Canal summer ■ Worldwide
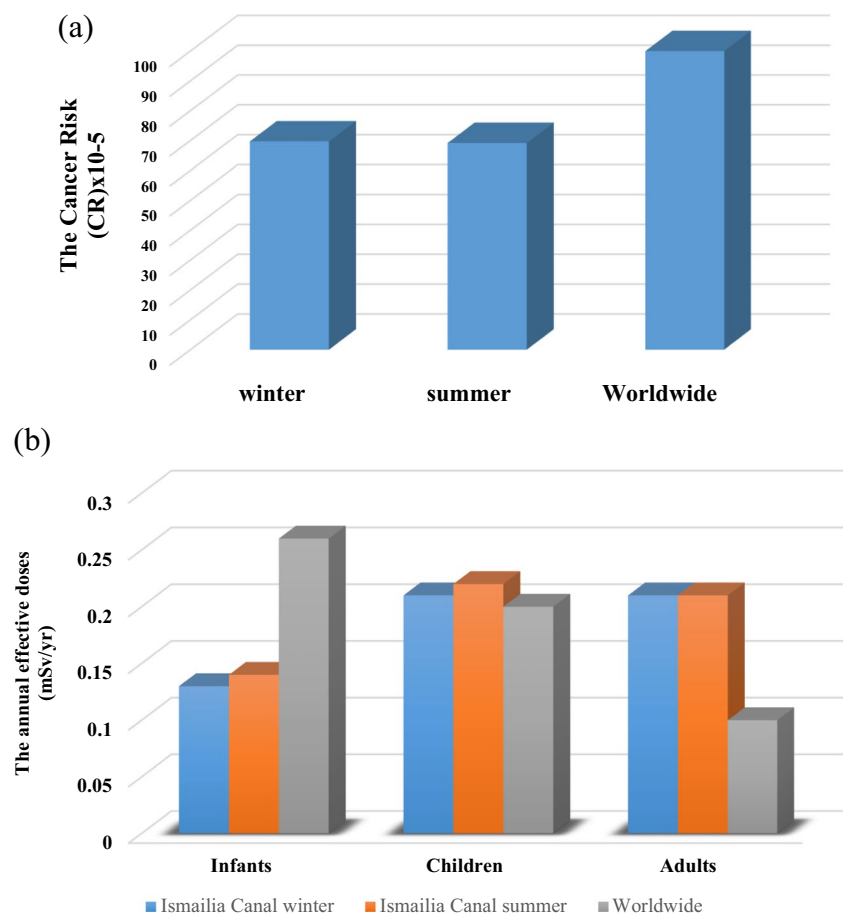
discharge of untreated domestic sewage, agricultural run-off, and industrial effluent. This investigation aimed to assess the impact of industrial contaminants on the water quality, radioactivity levels, and biological composition and distribution (attached diatoms) in the Ismailia Canal. Furthermore, the pollutants' environmental impact and health hazard indices in the Ismailia Canal are monitored. The anthropogenic disturbance plays a significant role in the biodiversity of aquatic biological communities, influencing species richness, evenness, ecological status, and fluctuation of radioactivity levels in the Ismailia Canal. This study showed that the BOD and COD values were only moderately clean, indicating higher levels of organic pollutants in surface waters. The WQI showed that the canal's water quality was unstable and ranged from 88 (good) to 97 (excellent) for drinking water. WQI values for aquatic and irrigation water range from 96–99 and 97–92, meeting WHO and Egyptian guidelines. Furthermore, the activity concentrations of ^{226}Ra, ^{232}Th, and ^{40}K in the water and sediment samples for both seasons remain within the permissible limits for natural radionuclides, except for some sites in the zone [B] (the industrial zone), which exceeded the guideline value. The fertilizer samples show higher ^{226}Ra activity in the raw material samples than in the commercial fertilizers (SSP and PCS).

Pollution impacts the diversity of diatoms, altering the structure and abundance of diatom communities, as indicated by the analysis of the diatom data. The total number of diatoms/cm³ and species were significantly reduced at the pollution discharge sites, contrasting with the residential areas, contributing to the high diatom densities and species richness. These areas boost the amount of nutrients at the limit that support algal growth and flourishing. The ecological tolerance of some diatom species to radionuclide activity was demonstrated concerning the distribution and ecological preferences of diatom species, as revealed by the respective differences in richness, evenness, and Shannon's diversity indices. The tolerance of microalgae assemblages to water quality parameters changed with industrial discharges, demonstrating the relevance of diatoms as biological indicators for this type of pollution. This association may involve the bioaccumulation of these radionuclides in diatom cells or their uptake into their metabolism. Consequently, these responses of some diatom species may allow further studies to use them in the phycoremediation process, which may be a promising opportunity in the water treatment in the Ismailia Canal. Multivariate redundancy analysis (RDA), explicitly examining ecological characteristics, radionuclides, and

the diatom community, showed that the unaffected sites differed significantly from those affected.

The radiological hazard index of the water, including the risk of cancer, falls within the USEPA ranges. The effective radiation doses from water consumption for infants and children are below the permissible limits, though higher for adults. Regarding sediment, the radium equivalent activities (Ra$_{eq}$), outdoor annual effective doses (E_{eff}), external hazard index (H_{ex}), and representative level index ($I\gamma$) were listed below the advised maximum levels for both seasons. Consequently, to improve the water quality of the canal,

the following technical recommendations are proposed: (1) To provide valuable data and information to communities and decision-makers, further in-depth long-term studies on physicochemical parameters, biological and radioactive levels of canal water, and eco-smart water treatment technologies should be carried out with the active participation of the local community; (2) promote waste reduction at source by enforcing existing laws and standards on pollution control and waste management; and (3) raise awareness among the people about the canal's importance in the pollution of the Nile River.

Appendix

Table 10 Quality control of radioactivity measurements comparison between measured values with certified reference values (Bq/kg)

Sample code	This analysis measured values (Bq/kg)			Certified reference values (Bq/kg)		
	^{226}Ra	^{232}Th	^{40}K	^{226}Ra	^{232}Th	^{40}K
IAEA-446	9.89 ± 0.5	11.1 ± 0.98	0.46 ± 0.3	9.34	10.5	0.44
IAEA-443	0.04 ± 0.002	0.05 ± 0.009	0.00188 ± 0.0002	0.039 ± 0.002	0.044 ± 0.002	0.00185 ± 0.0001
IAEA-410	10.4 ± 0.93	10.2 ± 1.3	-	10.1 ± 0.8	10.0 ± 1	-
IAEA-312	273.5	378.23	-	269	371.08	-

Table 11 CCME-WQI categories

Rating	CCME-WQI value	Remarks
Excellent	95–100	Water quality is protected with a virtual absence of threat or impairment; conditions very close to natural or pristine levels
Good	80–94	Water quality is protected with only a minor degree of threat or impairment; conditions rarely depart from natural or desirable levels
Fair	65–79	Water quality is usually protected but occasionally threatened or impaired; conditions sometimes depart from natural or desirable levels
Marginal	45–64	Water quality is frequently threatened or impaired; conditions often depart from natural or desirable levels
Poor	0.0–44	Water quality is almost always threatened or impaired; conditions usually depart from natural or desirable levels

Table 12 Radiation hazard indices and the health effect equations

Hazard indices	Equation	References
Absorbed dose rate in air (nGy/h)	$D = 0.462\, C_{Ra} + 0.621\, C_{Th} + 0.0417\, C_K$	UNSCEAR (2000)
Annual effective dose rates (mSv/year)	$\text{AED} = D \text{ (nGy/h)} \times 8760 \text{ (h/year)} \times 0.7 \text{ (Sv/Gy)} \times 0.2 \times 10^{-6}$	UNSCEAR (2000)
Radium equivalent activity (Bq/kg)	$\text{Ra}_{eq} = C_{Ra} + 1.43\, C_{Th} + 0.077\, C_K$	Kurnaz et al. (2007)
External hazard index (H_{ex})	$H_{ex} = (C_{Ra}/370 + C_{Th}/259 + C_K / 4810 \leq 1$	UNSCEAR (2000)
Representative level index (Bq/kg)	$I\gamma = \frac{C_{Ra}}{150} + \frac{C_{Th}}{100} + \frac{C_K}{1500}$	Chad-Umoren and Umoh (2017)
Cancer risk	$(CR) = MCL \times RC \times TWI$	EPA (1999); Abdellah and Diab (2012)
The effective radiation doses	$\text{DRW} = \text{AW} \times \text{IRW} \times \text{IDF}$	USEPA (1999)

C_{Ra}, C_{Th}, and C_K are the activity concentrations in becquerel per kilogram of ^{226}Ra, ^{232}Th, and ^{40}K, respectively. The conversion coefficient from absorbed dose to effective dose is 0.7 Sv/Gy, and the outdoor occupancy factor is 0.2.

Declarations

References

Abdel Malik WEY, Ibrahim AS, Youssef SK, Aziz M, El-Shinawy RMK (2010) Radiological review studies on ismailia canal ecology. Tenth Radiation Physics & Protection Conference, Nasr City - Cairo, Egypt

Abdel-Aal EI, Haroon AM, Ibrahim SM et al (2023) Ecological status of Lake Nasser Khors, Egypt, before operating the Grand Ethiopian Renaissance Dam. Stoch Environ Res Risk Assess 37:1229–1245. https://doi.org/10.1007/s00477-022-02329-5

Abdel-Satar AM, Ali MH, Goher ME (2017) Indices of water quality and metal pollution of Nile River, Egypt. Egypt J Aquat Res 43(1):21–29. https://doi.org/10.1016/j.ejar.2016.12.006

Abdellah WM, Diab HM (2012) Determination of natural radioactivity in drinking water and consequent dose to public. Nature and Science 10(1):137–142

Abdo MH, El-Nasharty SM (2010) Physico-chemical evaluations and trace metals distribution in water-surficial sediment of Ismailia Canal, Egypt. Nat Sci 8(5):198–206

El Afifi EM, Hilal MA, Khalifa SM, Aly HF (2006) Evaluation of U,Th,K and emanated radon in some NORM and TENORM samples. Journal of Radiation Measurment 41:627–633

Alam MN, Chowdhury MI, Kamal M, Ghose S, Banu H, Chakraborty D (1997) Radioactivity in chemical fertilizers used in Bangladesh. Appl Radiat Isot 48:1165–1168

ANS (2002) Protocols for the analysis of algal samples col- lected as part of the U.S. Geological Survey National Water-Quality Assessment Program, 02–06. https://water.usgs.gov/nawqa/protocols/algprotocol/index.html. Accessed 29 Apr 2021

APHA (1995) American public health association ''APHA'' Standard methods for the examination of water and waste water. Washington, D.C. USA, 19th edn. p 698

Asaduzzaman Kh, Khandaker MU, Amin YM, Bradley DA (2016) Natural radioactivity levels and radiological assessment of decorative building materials in Bangladesh. Indoor Built Environ 25(3):541–550. https://doi.org/10.1177/1420326X14562048

Badawy WM, Soliman NF, Eissa HS, Mahmoud AW (2015) Natural radioactivity and the associated dose from the terrestrial ecosystem of Ismailia Canal - Egypt. Int J Adv Res 3(1):779–788

Banerjee S, Kundu A, Dhak P (2022) Bioremediation of uranium from waste effluents using novel biosorbents: a review. J Radioanal Nucl Chem 1–27

Bastos RO, Appoloni CR (2009) Radio activity of rocks from the geological formations belonging to the Tibagi River Hydrographic Basin

Begum A, Hari Krishna S, Khan I, Ramaiah H, Veena K, Vinuta K (2008) Analysis of fluoride level in water and fish samples of Sankey, Bellandur and Madivala lakes of Bangalore, Karnataka. Rasayan J Chem 1(3):596–601

Belal D (2012) Epipelic diatoms as a tool for monitoring pollution in River Nile from Aswan to Cairo. M. Sc. Thesis. Fac. Sci. Cairo Univ., Egypt, p 109

Belivermis M, Kılıç Ö, Çotuk Y et al (2010) The effects of physico-chemical properties on gamma emitting natural radionuclide levels in the soil profile of Istanbul. Environ Monit Assess 163:15–26. https://doi.org/10.1007/s10661-009-0812-1

Bolívar JP, García-Tenorio R, García-León M (1996) Enhancement of natural radionuclides in soils and salt-marshes surrounding a non-nuclear industrial complex. Sci Total Environ 173(174):125–136

Bolivar JP, Garcia-Tenorio R, Vaca F (2000) Radioecological study of an estuarine system located in the south of Spain. Water Res 34:2941e2950

Brigden K, Stringer R, Santillo D (2002) Heavy metal and radionuclide contamination of fertilizer products and phosphogypsum waste produced by the Lebanese chemical company, Lebanon, Greenpeace Research Laboratories, Technical Note 13

Camacho A, Montaña M, Vallés I, Devesa R, Céspedes-Sánchez R, Serrano I, Blázquez S, Barjola V (2012) Behavior of natural radionuclides in wastewater treatment plants. J Environ Radioact 109:76–83. https://doi.org/10.1016/j.jenvrad.2012.02.005

Canadian Council of Ministers of the Environment (2001) Canadian water quality guidelines for the protection of aquatic life: CCME Water Quality Index 1.0, Technical Report. In: Canadian environmental quality guidelines, 1999, Canadian Council of Ministers of the Environment, Winnipeg

CCME (2007) Canadian Council of Ministers of the Environment For the protection of aquatic life. In: Canadian Environmental

Quality Guidelines, 1999, Canadian Council of Ministers of the Environment, 1999, Winnipeg

Chad-Umoren YE, Umoh IJ (2017) A gamma spectrometric analysis and radium equivalent activity index of water in ABAK, Nigeria: a base- line survey.Environ. Earth Sci 7(5):19–26

Chauhan P, Chauhan RP, Gupta M (2013) Estimation of naturally occurring radionuclides in fertilizers using gamma spectrometry and elemental analysis by XRF and XRD techniques. Microchem J 106:73–78. https://doi.org/10.1016/j.microc.2012.05.007

Chieco NA, Bogen DC, Knutson EO (1990) Environmental measurements laboratory (EML) procedures manual

Chu T, Wang J (2000) Radioactive disequilibrium of uranium and thorium nuclide series in hot spring and river water from Peitou Hot Spring Basin in Taipei 1(1)

Clarke K, Gorley R (2001) PRIMER v5: user manual, PRIMER-E, Plymouth UK, p 91

Cleve-Euler A (1953) Die Diatomeen von Schweden und Finland. Band 1, 2, 3, 4 and 5. Stockholm, Almqvist and Wiksells B oktryckeri AB

Dajawa D, Goswami AK, Laskar I (2009) Radon exhalation rate studies in Makum coalfield area using track-etched detectors. Indian J Phys 83(8):1155–1162

Edsfeldt C (2001) The radium distribution in some swedish soils and its effect on radon emanation the radium distribution in some Swedish

Eisenbud M, Gesell T (1997) Environmental radioactivity from natural, industrial, and military sources. Academic Press, London, p 656

El Bouraie MM, El Barbary AA, Yehia MM, Motawea EA (2010) Heavy metal concentrations in surface river water and bed sediments at Nile Delta in Egypt. Suo 61(1):1–12

El Sayed SM, Hegab MH, Mola HRA et al (2020) An integrated water quality assessment of Damietta and Rosetta branches (Nile River, Egypt) using chemical and biological indices. Environ Monit Assess 192:228. https://doi.org/10.1007/s10661-020-8195-4

El Sayed SM, Aly MY, El-Shamy AS, El-Gaar DMK, Ghallab MH (2023) Water quality indices and risk assessment of consumption of nile tilapia tissues from Ismailia Canal, Egypt. Egypt J Aquat Bio Fish 27(2):305–324

El-Gamal H, Sefelnasr A, Salaheldin G (2019) Determination of natural radionuclides for water resources on the west bank of the Nile River, Assiut Governorate, Egypt. Water (Switzerland) 11(2). https://doi.org/10.3390/w11020311

El-Gamal H, Sefelnasr A, Salaheldin G (2019) Determination of natural radionuclides for water resources on the west bank of the nile river, assiut governorate, Egypt. Water (Switzerland), 11(2). https://doi.org/10.3390/w11020311

El-Haddad ESM (2005) Some Environmental Studies on Water and Sediment of Ismailia Canal from El Mazalat to Anshas Region. M.Sc. Thesis, Faculty of Science (Girl Branch) Al Azhar University

Elizabeth ER, Phillips JP (2001) Sulfate-reducing bacteria release barium and radium from naturally occurring radioactive material in oil-field barite. Geomicrobiol J 18:167–182

El-Mathana ME, Mostafa NG, Galal MM, Elawwad A (2021) Assessment and simulation of a solid waste dumpsite impact on the surrounding water resources: a case study in Abu Zaabal, Egypt. Heliyon 7(11):e08421. https://doi.org/10.1016/j.heliyon.2021.e08421

El-Reefy HI, Sharshar T, Elnimr T, Badran HM (2010) Distribution of gamma-ray emitting radionuclides in the marine environment of the Burullus Lake: II. Bottom Sediments. Environ Monit Assess 169(1–4):273–284. https://doi.org/10.1007/s10661-009-1169-1

El-Sayed SMM (2011) Physicochemical studies on the impact of pollution up on the Nile River branches. Thesis Faculty of Science, Benha University, Egypt, Egypt. M.Sc

Elsayed FA, Okbah MA, El-Syed SM, Eissa MA, Goher ME (2019) Nutrient salts and eutrophication assessment in northern delta lakes: case study Burullus Lake, Egypt. Egypt J Aquat Biol Fish 23(2):145–163

El-Taher A, Abdelhalim MAK (2013) Elemental analysis of phosphate fertilizer consumed in Saudi Arabia. Life Sci J 10(4):701–708

El-Taher A, Makhluf S (2010) Natural radioactivity levels in phosphate fertilizer and its environmental implications in Assuit Governorate, upper Egypt. Indian J Pure Appl Phys 48(10):697–702

Enache M, Prairie YT (2002) WA-PLS diatom-based pH, TO, and DOC inference models from 42 lakes in the Abitibi clay belt area (Quebec, Canada). J Paleolimnol 27:151–171

EWQS (Egyptian drinking water quality standards) (2007) Ministry of Health, Population Decision number 458

Falasco E, Blanco S, Bona F, Goma J, Hlubikova D, Novais MH, Hoffmann L, Ector L (2009) Taxonomy, morphology and distribution of the Sellaphora stroemii complex (Bacillariophyceae). Fottea 9(2):243–256

FAO 1994. Water quality for agriculture, irrigation and drainage. In: Ayers RS, Westcot DW (eds.) Food, Agriculture Organization of the United Nations, Rome. Paper 29, Rev 1

Geriesh MH, Balke KD, El-Rayes AE (2008) Problems of drinking water treatment along Ismailia Canal Province, Egypt. J Zhejiang Univ: Sci B 9(3):232–242. https://doi.org/10.1631/jzus.B0710634

Goher ME, Hassan AM, Abdel-Moniem IA, Fahmy AH, El-Sayed SM (2014) Evaluation of surface water quality and heavy metal indices of Ismailia Canal, Nile River, Egypt. Egypt J Aquat Res 40:225–233

Goher ME, Abdo MH, Mangood AH, Hussein MM (2015) Water quality and potential health risk assessment for consumption of Oreochromis niloticus from El-Bahr El-Pharaony Drain, Egypt. Fresenius Environ Bull 24(11):3590–3602

Goher ME, Napiórkowska-Krzebietke A, Aly W et al (2021) Comprehensive insight into Lake Nasser environment: water quality and biotic communities—a case study before operating the renaissance dam. Water 13(16):2195. https://doi.org/10.3390/w13162195

Heidari F, Riahi H, Aghamiri MR, Shariatmadari Z, Zakeri F (2017) Isolation of an efficient biosorbent of radionuclides (^{226}Ra, ^{238}U): green algae from high-background radiation areas in Iran. J Appl Phycol 29:2887–2898

Hussein EM (1994) Radioactivity in phosphate ore, super phosphate, and phosphogypsum in Abu-Zaabal phosphate plant Egypt. Health Phys 67(3):280–282

HusseinM M, Goher ME, Mangood AH, Mousa IE (2023) Water quality profile and metal pollution indices of the main stream of the Nile River in Egypt. Afr J Aquat Sci 48(2):138–151. https://doi.org/10.2989/16085914.2023.2188165

IAEA (1996) International basic safety standards for protection against ionizing radiation and for the safety of radiation sources. Safety Series 15, Vienna

Ibrahim SS, Bakery HH, El-shawarby R, Abuo Salem M, Nabila M (2014) Incidence of some pollutants in Ismailia Canal and using different methods for removal. Benha Vet Med J 27(1):62–77

International Atomic Energy Agency (IAEA) (1987) Advisory material for the IAEA regulations for the safe transportof radioactive material (1985 edn) safety series 3, 3rd edn (Vienna: IAEA)

International Atomic Energy Agency (2014) The environmental behaviour of radium: revised edition. Technical reports series no. 476

Imam N, El-sayed SM, Goher ME (2020) Risk assessments and spatial distributions of natural radioactivity and heavy metals in Nasser Lake, Egypt. Environ Sci Pollut Res 27(20):25475–25493. https://doi.org/10.1007/s11356-020-08918-7

Kandil AT, Haggag K, Gamal AA, Abd El-Nasser MG, Mostafa WM (2023) Adverse health and environmental outcomes of sewage treatment plant on surrounding groundwater with emphasis on some mitigation recommendations. Environ Geochem Health 45(6):3345–3359. https://doi.org/10.1007/s10653-022-01413-7

Khan K, Khan HM, Tufail M, Khatibeh AJAH, Ahmad N (1998) Radiometric analysis of Hazara phosphate rock and fertilizers in Pakistan. J Environl Radioact 38(1):77–84

Kim Y (1995) Aquifer mineralogy and natural radionuclides in groundwater: the lower Paleozoic of central Texas. Texas A&M University

Krammer K, Lange-Bertalot H (1986) Bacillariophyceae. Teil: Naviculaceae. Susswasserflora von Mitteleuropa, 2/1: 1-876. Gustav Fisher Verlag, Stuttgart, Germany

Krammer K, Lange-Bertalot H (1988) Bacillariophyceae 1. Teil: Bacillariaceae, Epithemiaceae, Surirellaceae. Susswasserflora von Mitteleuropa, 2/'2: 1-596. Gustav Fisher Verlag, Stuttgart, Germany

Krammer K, Lange-Bertalot H (1991) Bacillariophyceae 3. Teil: Centrales, Fragillariaceae, Eunotiaceae. Susswasserflora von Mittelenropa, 2/3: 1-576. Gustav Fisher Verlag, Stuttga

Kurnaz A, Kucukomeroglu B, Keser R, Okumusoglu NT, Korkmaz F, Karahan G, Cevik U (2007) Determination of radioactivity levels and hazards of soil and sediment samples in Fırtına Valley (Rize, Turkey). Appl Radiat Isot 65:1281–1289

Li L, Pan C, Ling S, Li M (2022) Ecological efficiency of urban industrial land in metropolitan areas: evidence from China. Land 11(1). https://doi.org/10.3390/land11010104

El Mamoney MH, Khater AEM (2004) Environmental characterization and radio-ecological impacts of non-nuclear industries on the Red Sea coast. 73:151–168. https://doi.org/10.1016/j.jenvrad.2003.08.008

Manigandan PK, Chandar Shekar B (2014) Evaluation of radionuclides in the terrestrial environment of Western Ghats. J Radiat Res Appl Sci 7(3):310–316. https://doi.org/10.1016/j.jrras.2014.04.001

Menzie CA, Southworth B, Stephenson G, Feisthauer N (2008) The importance of understanding the chemical form of a metal in the environment: The case of barium sulfate (barite). Hum Ecol Risk Assess 14:974–991

Millan F, Izere C, Breton V, Voldoire O, Biron DG, Wetzel CE, Miallier D, Allain E, Ector L, Beauger A (2020) The effect of natural radioactivity on diatom communities in mineral springs. Bot Lett 167(1):95–113. https://doi.org/10.1080/23818107.2019.1691051

Mohamed MH (2021) Implications of applied p-sources with calcium super phosphate, phosphoric acid and rock phosphate, and phosphate dissolving bacteria on snap bean grown under greenhouses conditions. Ann Agric Sci Moshtohor 59(5):697–710. https://doi.org/10.21608/assjm.2021.195424

Mourad NM, Sharshar T, Elnimr T, Mousa MA (2009) Radioactivity and fluoride contamination derived from a phosphate fertilizer plant in Egypt. Appl Radiat Isotopes 67:1259–1268

Ndiritu GG, Gichuki NN, Triest L (2006) Distribution of epilithic diatoms in response to environmental conditions in an urban tropical stream, Central Kenya. Biodivers Conserv 15:3267–3293. https://doi.org/10.1007/s10531-005-0600-3

Pappa KF, Tsabaris C, Ioannidou A, Patiris LD, Kaberi H (2016) Radioactivity and metal concentrations in marine sediments associated with mining activities in Ierissos Gulf, North Aegean Sea, Greece. Appl Radiat Isot 116:22–33

Patrick R, Reimer CW (1975) The diatoms of the United States, exclusive of Alaska & Hawaii. Academy of Natural Sciences. Philadelphia, vol. U, p 213

Poonam T, Tanushree B, Sukalyan C (2013) Water quality indices-important tools for water quality assessment: a review. Int J Adv Chem (IJAC) 1(1):15–28

Pradhan D, Sukla LB (2019) Removal of radon from radionuclide-contaminated water using microalgae. In: Sukla L, Subudhi E, Pradhan D (Eds.) The Role of Microalgae in Wastewater Treatment. Springer, Singapore, pp 75–86

Ramadan AB, Atomic E, Authority E, Nuclear E, Authority RR, Helmy M, Monged E (2015) Evaluation of physico-chemical characteristics and natural radioactivity for water quality of Ismailia Canal , Egypt

Renock D, Landis JD, Sharma M (2016) Reductive weathering of black shale and release of barium during hydraulic fracturing. Appl Geochem 65:73–86

Righi S, Betti M, Bruzzi L, Mazzotti G (2000) Monitoring of natural radioactivity in working places. Microchem J 67:119–126

Saueia CH, Mazzilli BP, Favaro DI (2005) Natural radioactivity in phosphate rock, phosphogypsum and phosphate fertilizers in Brazil. Radioanal Nucl Chem 264(2):445–448

Sherwood AR, Rintoul TL, Muller KM, Sheath RG (2000) Seasonality and distribution of epilithic diatoms, macroalgae and macrophytes in a spring-fed stream system in Ontario, Canada. Hydrobiologia 435:143–152

Sukla L, Subudhi E, Pradhan D (eds) (2019) The role of microalgae in wastewater treatment. Springer, Singapore. https://doi.org/10.1007/978-981-13-1586-2_1

Talab AS, Goher ME, Ghannam HE, Abdo MH (2016) Chemical compositions and heavy metal contents of Oreochromis niloticus from the main irrigated canals (Rayahs) of Nile Delta. Egypt J Aquat Res 42:23–31

Taskin H, Karavus M, Ay P, Topuzoglu A, Hindiroglu S, Karahan G (2009) Radionuclide concentrations in soil and lifetime cancer risk due to the gamma radioactivity in Kirklareli, Turkey. J Environ Radioact 100:49–53

Ter Braak C (1987) The analysis of vegetation-environment relationships by canonical correspondence analysis. Vegetation 69:69–77

Ter Braak CJF, Smilauer P (2002) Canoco 4.5 software for canonical community ordi_nation. Microcomputer Power, Ithaca NY, US

Turekian KK, Wedepohl KH (1961) Distribution of the elements in some major units of the Earth's crust. Geol Soc Am Bull 72:175–192

United States Department of Energy (USDOE) (1992) EML procedures manual, Report HASL 300. WHO, World Health Organization. In: 2003 Guidelines for drinking water quality, vol. 3. -Chapter 9 draft, Geneva, Switzerland

UNSCEAR (2000) Sources, effects and risks of ionizing radiations. United Nations

USEPA (2000) Quality criteria for water. EPA 440/5-86-001. 2001. Office of water regulations and standards. Washington DC, USA

USEPA, United States Environmental Protection Agency (1999) Final draft for the drinking water criteria document on radium. Washington, Dc, 1999 Tr-1241- 85

Utermohl H (1958) Zur vervollkommung der quantitativen phytoplankton-methodik. Internationale Vereinigung fur Theoretische 'and Angewandte Limnologie 9:1–38

Van Dam H, Mertens A, Sinkeldam J (1994) A coded checklist and ecological indicator values of freshwater diatoms from the Netherlands. Neth J Aquat Ecol 28(1):117–133

Wang B, Liu C, Wang F, Chetelat B, Maberly SC (2013) Diatoms modify the relationship between dissolved silicon and bicarbonate in impounded rivers. J Limnol 72(3):494–504. https://doi.org/10.4081/jlimnol.2013.e40

WHO, World Health Organization (2003) Guidelines for drinking water quality, vol.3-Chapter 9 draft, Geneva, Switzerland

WHO (2011) Guidelines for drinking water quality, fourth ed. Geneva: WHO, 564p. ISBN: 978 92 4154815 1

Youssef SK, Ibrahim AS, Malik WEYA, Seifin SM (2004) Physico-chemical and radiological studies on some egyptian aquatic areas. VII Radiation Physics & Protection Conference, 27-30 November 2004, Ismailia-Egypt, pp 27–30

Publisher's Note Springer Nature remains neutral with regard to jurisdictional claims in published maps and institutional affiliations.